Image decomposition: application to textured images and SAR images

Jean-François Aujol, Gilles Aubert, Laure Blanc-Féraud, Antonin Chambolle

INRIA

INSTITUT NATIONAL DE RECHERCHE EN INFORMATIQUE ET EN AUTOMATIQUE

Image decomposition: application to textured images and SAR images.

Jean-François Aujol — Gilles Aubert — Laure Blanc-Féraud — Antonin Chambolle

N° 4704

January 2003

THÈME 3

ISSN 0249-6399

INRIA
SOPHIA ANTIPOLIS

Image decomposition: application to textured images and SAR images.

Jean-François Aujol [*] [†] , Gilles Aubert [‡] [§] , Laure Blanc-Féraud [¶] , Antonin Chambolle [‖] [**]

Thème 3 — Interaction homme-machine,
images, données, connaissances
Projet Ariana

Rapport de recherche n° 4704 — January 2003 — 53 pages

Abstract: In this report, we present a new algorithm to split an image f into a component u belonging to BV and a component v made of textures and noise of the initial image. We introduce a functional adapted to this problem. The minimum of this functional corresponds to the image decomposition we want to get. We compute this minimum by minimizing successively our functional with respect to u and v. We carry out the mathematical study of our algorithm. We present some numerical results. On the one hand, we show how the v component can be used to classify textured images, and on the other hand, we show how the u component can be used in SAR image restoration.

[*] également membre du laboratoire J.A Dieudonné, Université de Nice-Sophia-Antipolis
[†] jfaujol@sophia.inria.fr
[‡] Laboratoire J. A. Dieudonné, UMR CNRS 6621, Université de Nice-Sophia-Antipolis, Parc Valrose, 06108 Nice Cedex 2, France
[§] gaubert@math.unice.fr
[¶] blancf@sophia.inria.fr
[‖] CEREMADE, CNRS UMR 7534, Université Paris IX - Dauphine, Place du Maréchal De Lattre De Tassigny, 75775 Paris Cedex 16, France
[**] antonin.chambolle@ceremade.dauphine.fr

Unité de recherche INRIA Sophia Antipolis
2004, route des Lucioles, BP 93, 06902 Sophia Antipolis Cedex (France)
Téléphone : +33 4 92 38 77 77 —Télécopie : +33 4 92 38 77 65

Key-words: Total variation minimization, BV, texture, classification, restoration, SAR images, speckle

Décomposition d'images: application aux images texturées et aux images RSO.

Résumé : Dans ce rapport, nous présentons un nouvel algorithme pour décomposer une image$f$ en $u+v$, u étant à variation bornée, et v contenant les textures et le bruit de l'image originale. Nous introduisons une fonctionnelle adaptée à ce problème. Le minimum de cette fonctionnelle correspond à la décomposition cherchée de l'image. Le calcul de ce minimum se fait par minimisation successive par rapport à chacune des variables, chaque minimisation étant réalisée à l'aide d'un algorithme de projection. Nous faisons l'étude théorique de notre modèle, et nous présentons des résultats numériques. D'une part, nous montrons comment la composante v peut être utilisée pour faire de la classification d'images texturées, et d'autre part nous montrons comment la composante u peut être utilisée en restauration d'images SAR.

Mots-clés : Minimisation de la variation totale, BV, texture, classification, restauration, images RSO, speckle

Contents

List of Figures

1. Introduction

1.1 Preliminaries

Image restoration is one of the major goals of image processing. A classical approach consists in considering that an image f can be decomposed into two components $u+v$. The first component u is well-structured, and has a simple geometric description: it models the homogeneous objects which are present in the image. The second component v contains both textures and noise. An ideal model would split an image into three components $u+v+w$, where v should contain the textures of the original image, and w the noise.

In Section 1, we begin by recalling some models proposed in the literature. Then our model is introduced in Section 2. We give a powerful algorithm to compute the image decomposition we want to get. We carry out the mathematical study of our model in Section 3. We then show some experimental results. We compare the total variation minimization algorithm with our approach in Section 4. In Section 5, we give a first application by using the v component to classify textured images. In Section 6, we give an application to SAR images, the u component being a way to carry out efficient restoration.

1.2 Related works

1.2.1 Rudin-Osher-Fatemi's model

Images are often assumed to be in BV, the space of functions with bounded variation (even if it is known that such an assumption is too restrictive [1]). We recall here the definition of BV:

Definition 1.1. $BV(\Omega)$ is the subspace of functions $u \in L^1(\Omega)$ such that the following quantity is finite:

$$J(u) = \sup \left\{ \int_\Omega u(x) \mathrm{div}\,(\xi(x)) dx / \xi \in C_c^1(\Omega;\mathbb{R}^2), \|\xi\|_{L^\infty(\Omega)} \leq 1 \right\} \qquad (1.1)$$

$BV(\Omega)$ endowed with the norm $\|u\|_{BV} = \|u\|_{L^1} + J(u)$ is a Banach space.

If $u \in BV(\Omega)$, the distributional derivative Du is a bounded Radon measure and (1.1) corresponds to the total variation of $|Du|(\Omega)$.

In [13], the authors decompose an image f into a component u belonging to $BV(\Omega)$ and a component v in $L^2(\Omega)$. In this model v is supposed to be the noise.

In such an approach, they minimize (see [13]):

$$\inf_{(u,v)\in BV(\Omega)\times L^2(\Omega)/f=u+v} \left(J(u) + \frac{1}{2\lambda}\|v\|_2^{L^2(\Omega)} \right) \tag{1.2}$$

In practice, they try to compute a numerical solution of the Euler-Lagrange equation associated to (1.2). The mathematical study of (1.2) has been done in [4].

1.2.2 Meyer's model

In [9], Y. Meyer proposes a different decomposition. He shows that the model in [13] does not reach its aim. In particular, if $f = \chi_\Omega$ where Ω is a bounded domain with a C^∞-boundary, then f is not preserved by the Rudin-Osher-Fatemi model (contrary to what should be expected). Instead, he proposes the following model:

$$\inf_{(u,v)\in BV(\mathbb{R}^2)\times G(\mathbb{R}^2)/f=u+v} (J(u) + \lambda\|v\|_G) \tag{1.3}$$

The Banach space $G(\mathbb{R}^2)$ contains signals with strong oscillations, and thus in particular textures and noise.

We give here the definition of $G(\mathbb{R}^2)$.

Definition 1.2. $G(\mathbb{R}^2)$ is the Banach space composed of the distributions f which can be written

$$f = \partial_1 g_1 + \partial_2 g_2 = \operatorname{div}(g) \tag{1.4}$$

with g_1 and g_2 in $L^\infty(\mathbb{R}^2)$.

On G, the following norm is defined:

$$\begin{aligned}\|v\|_G &= \inf\Big\{\|g\|_{L^\infty(\mathbb{R}^2)} = \operatorname*{ess\,sup}_{x\in\mathbb{R}^2}|g(x)| \ / v = \operatorname{div}(g),\\ &\qquad g=(g_1,g_2), g_1\in L^\infty(\mathbb{R}^2), g_2\in L^\infty(\mathbb{R}^2),\\ &\qquad |g(x)| = \sqrt{|g_1|^2+|g_2|^2}(x)\Big\} \end{aligned} \tag{1.5}$$

The justification of the introduction of the space G to model patterns with strong oscillations comes from the next result (see [9]):

Lemma 1.1. *let f_n , $n \geq 1$ a sequence of functions in $L^2(D)$ with the three following properties (D is a disc centered at 0 with radius R):*

1. *There exists a compact set K such that the supports of the f_n, $n \geq 1$ are embedded in K.*
2. *There exists $q > 2$ and $C > 0$ such that $\|f_n\|_q \leq C$*
3. *The sequence f_n converges to 0 in the distributional sense.*

Then $\|f_n\|_G$ converges to 0 when n tends towards infinity.

This lemma tells us that a signal f may be of relatively large norm $\|.\|_q$, whereas $\|f\|_G$ is very close to 0.

1.2.3 Vese-Osher's model

L. Vese and S. Osher have tried to realize Meyer's program. They have studied the problem (see [17]):

$$\inf_{(u,v)\in BV(\Omega)\times G(\Omega)}\left(\int |Du| + \lambda\|f-u-v\|_2^2 + \mu\|v\|_{G(\Omega)}\right) \tag{1.6}$$

where Ω is a bounded open set.

To compute their solution, they formally derive the Euler-Lagrange equations from (1.6), and the term $\|v\|_{G(\Omega)}$ is replaced by:

$$\|\sqrt{g_1^2+g_2^2}\|_p \tag{1.7}$$

(where $v = \mathrm{div}\,(g_1, g_2)$).

It is true that when $p \to +\infty$, (1.7) tends towards $\|\sqrt{g_1^2 + g_2^2}\|_\infty$.

But in practice, for numerical reasons, the authors use the value $p = 1$. Nevertheless, they report good numerical results. But actually they do not solve Meyer's problem.

These two authors, together with A. Solé, have proposed another approach to this problem in [11].

2. Our approach

In this section we introduce our model. We first formulate it in the continuous-setting. Then we propose a discretization, and provide a mathematical study and an algorithm for the discretized model.

2.1 Presentation

We propose to solve the problem:

$$\inf_{(u,v)\in BV(\Omega)\times G_\mu(\Omega)} \left(J(u) + \frac{1}{2\lambda}\|f - u - v\|^2_{L^2(\Omega)} \right) \tag{2.1}$$

where

$$G_\mu(\Omega) = \{v \in G(\Omega) / \|v\|_G \leq \mu\} \tag{2.2}$$

We remind that $\|v\|_G$ is defined by (1.5).

The parameter μ plays the same role as the one in problem (1.6). We will precise the link of our model with Meyer's one later.

Let us introduce the following functional defined on $BV(\Omega) \times G(\Omega)$:

$$F(u,v) = \begin{cases} J(u) + \frac{1}{2\lambda}\|f - u - v\|^2_{L^2(\Omega)} & \text{if } v \in G_\mu(\Omega) \\ +\infty & \text{if } v \in G(\Omega)\backslash G_\mu(\Omega) \end{cases} \tag{2.3}$$

$F(u,v)$ is finite if and only if (u,v) belongs to $BV(\Omega) \times G_\mu(\Omega)$.

Problem (2.1) can thus be written:

$$\inf_{(u,v)\in BV(\Omega)\times G(\Omega)} F(u,v) \tag{2.4}$$

2.2 Discretization

We are now going to study (2.4) in the discrete case. We take here the same notations as in [3].

The image is a two dimension vector of size $N \times N$. We denote by X the Euclidean space $\mathbb{R}^{N\times N}$, and $Y = X \times X$. The space X will be endowed with the scalar product

$$(u, v)_X = \sum_{1\leq i,j\leq N} u_{i,j} v_{i,j} \tag{2.5}$$

and the norm

$$\|u\|_X = \sqrt{(u, u)_X} \tag{2.6}$$

To define a discrete total variation, we introduce a discrete version of the gradient operator. If $u \in X$, the gradient ∇u is a vector in Y defined by:

$$(\nabla u)_{i,j} = ((\nabla u)^1_{i,j}, (\nabla u)^2_{i,j}) \tag{2.7}$$

with

$$(\nabla u)^1_{i,j} = \begin{cases} u_{i+1,j} - u_{i,j} & \text{if } i < N \\ 0 & \text{if } i = N \end{cases} \tag{2.8}$$

$$(\nabla u)^2_{i,j} = \begin{cases} u_{i,j+1} - u_{i,j} & \text{if } j < N \\ 0 & \text{if } j = N \end{cases} \tag{2.9}$$

The discrete total variation of u is then defined by:

$$J(u) = \sum_{1\leq i,j\leq N} |(\nabla u)_{i,j}| \tag{2.10}$$

We also introduce a discrete version of the divergence operator. We define it by analogy with the continuous setting by

$$\text{div } = -\nabla^* \tag{2.11}$$

where ∇^* is the adjoint of ∇: that is, for every $p \in Y$ and $u \in X$, $(-\text{div}\, p, u)_X = (p, \nabla u)_Y$. It is easy to check that:

$$(\text{div}\,(p))_{i,j} = \begin{cases} p^1_{i,j} - p^1_{i-1,j} & \text{if 1<i<N} \\ p^1_{i,j} & \text{if i=1} \\ -p^1_{i-1,j} & \text{if i=N} \end{cases} + \begin{cases} p^2_{i,j} - p^2_{i,j-1} & \text{if 1<j<N} \\ p^2_{i,j} & \text{if j=1} \\ -p^2_{i,j-1} & \text{if j=N} \end{cases} \tag{2.12}$$

We are now in position to introduce the discrete version of the space G.

Definition 2.1.

$$G^d = \{v \in X \ / \ \exists g \in Y \text{ such that } v = \operatorname{div}(g)\} \tag{2.13}$$

and if $v \in G^d$:

$$\begin{aligned} \|v\|_{G^d} &= \inf \{\|g\|_\infty \ / \ v = \operatorname{div}(g), \\ &\qquad g = (g^1, g^2) \in Y, |g_{i,j}| = \sqrt{(g^1_{i,j})^2 + (g^2_{i,j})^2}\Big\} \end{aligned} \tag{2.14}$$

where $\|g\|_\infty = \max_{i,j} |g_{i,j}|$.

Moreover, we will denote:

$$G^d_\mu = \left\{v \in G^d \ / \ \|v\|_{G^d} \leq \mu\right\} \tag{2.15}$$

$\|.\|_{G^d}$ is closely linked with J.

Proposition 2.1.

$$J(u) = \sup_{v \in G^d_1} (u, v)_X \tag{2.16}$$

and

$$\|v\|_{G^d} = \sup_{J(u) \leq 1} (u, v)_X \tag{2.17}$$

We already know (2.16). To prove (2.17), we need the following lemma (which is stated in [9]).

Lemma 2.1. *Let $u \in X$ and $v \in G^d$. Then:*

$$(u, v)_X \leq J(u)\|v\|_{G^d} \tag{2.18}$$

Proof: Let $g \in Y$ such that $v = \operatorname{div}(g)$.

$$(u, v)_X = (u, \operatorname{div}(g))_X = -(\nabla u, g)_Y \leq J(u)\|v\|_{G^d} \tag{2.19}$$

And we deduce (2.18) from it.

■

We also need the next result:

Lemma 2.2. *$u \mapsto \frac{J(u)^2}{2}$ and $v \mapsto \frac{\|v\|^2_{G^d}}{2}$ are dual in the sense of the Legendre-Fenchel duality.*

Proof: We recall here (see [5, 12, 6]) the definition of the Legendre-Fenchel transform of H:

$$H^*(v) = \sup_{u \in X} \left((u,v)_X - H(u) \right) \tag{2.20}$$

We want to show that $u \mapsto \frac{J(u)^2}{2}$ and $v \mapsto \frac{\|v\|^2_{G^d}}{2}$ are dual with respect to this definition.

Let us denote by ϕ the function $\phi(t) = \frac{t^2}{2}$. It is well known that $\phi^* = \phi$.

$$\begin{aligned}
\left(\frac{\|.\|^2_{G^d}}{2} \right)^* (u) &= \sup_{v \in X} ((u,v)_X - \phi(\|v\|_{G^d})) \\
&= \sup_{t \geq 0} \sup_{\|v\|_{G^d} = t} ((u,v)_X - \phi(\|v\|_{G^d})) \\
&= \sup_{t \geq 0} \sup_{\|v\|_{G^d} = 1} ((u,tv)_X - \phi(t\|v\|_{G^d})) \\
&= \sup_{\|v\|_{G^d} = 1} \sup_{t \geq 0} (t(u,v)_X - \phi(t))
\end{aligned}$$

And since ϕ is even we get:

$$\begin{aligned}
\left(\frac{\|.\|^2_{G^d}}{2} \right)^* (u) &= \sup_{\|v\|_{G^d} = 1} \phi^*((u,v)_X) \\
&= \sup_{\|v\|_{G^d} = 1} \frac{(u,v)^2_X}{2} \\
&= \frac{1}{2} \left(\sup_{\|v\|_{G^d} = 1} (u,v)_X \right)^2
\end{aligned}$$

But

$$\sup_{\|v\|_{G^d} = 1} (u,v)_X = \sup_{\|v\|_{G^d} \leq 1} (u,v)_X \tag{2.21}$$

And we conclude with (2.16).

■

Proof of Proposition 2.1: We want to prove (2.17). Lemma 2.1 gives an inequality. Let us show the reverse inequality. We denote by ∂H the subdifferential of H (see [12, 6]), and we recall that

$$w \in \partial H(u) \Longleftrightarrow H(v) \geq H(u) + (w, v-u)_X \text{ , for all } v \text{ in } X \tag{2.22}$$

Let $v \in G^d$. We recall that (see [5]), if H is convex:

$$H(u) + H^*(v) = (u, v)_X \tag{2.23}$$

if and only if $u \in \partial H^*(v)$. We apply this result with $H^*(v) = \left(\frac{J(.)^2}{2}\right)^*(v)$. Since $\left(\frac{J(.)^2}{2}\right)^*$ is convex continuous, we know that $\partial H^*(v)$ is not empty. Let $u \in \partial H^*(v)$. From Lemma 2.2, we get:

$$\frac{J(u)^2}{2} + \frac{\|v\|^2_{G^d}}{2} = (u, v)_X \tag{2.24}$$

i.e:

$$\underbrace{\left(J(u) - \|v\|_{G^d}\right)^2}_{\geq 0} = 2\left((u, v)_X - J(u)\|v||_{G^d}\right) \tag{2.25}$$

Hence

$$(u, v)_X \geq J(u)\|v||_{G^d} \tag{2.26}$$

And this conclude the proof thanks to Lemma 2.1.

■

Proposition 2.2. *The space G^d identifies with the following subspace:*

$$X_0 = \{v \in X \ / \ \sum_{i,j} v_{i,j} = 0\} \tag{2.27}$$

Proof: We split our proof into two steps:
Step 1:
Let us assume that $v \in G^d$. Therefore, there exists $g \in Y$ such that:

$$v = \text{div}\,(g) \tag{2.28}$$

And

$$\sum_{i,j} (\text{div}\, g)_{i,j} = (-\nabla^* g, 1)_Y = (g, \nabla 1)_X = 0 \tag{2.29}$$

i.e. $v \in X_0$. Hence $G^d \subset X_0$.
Step 2:
Conversely, let $v \in X_0$. Since the kernel of ∇ is the constant images, i.e. the vectors $x \in X$ such that $x_{i,j} = x_{i',j'}$ for all i, j, i', j', it is clear that a discrete Poincaré inequality holds:

$$\|x - \frac{1}{N^2} \sum_{i,j} x_{i,j}\|_X \leq c \|\nabla x\|_Y \tag{2.30}$$

Hence one shows easily that the problem

$$\min_{x \in X} A(x) \tag{2.31}$$

with

$$A(x) = \|\nabla x\|^2 + 2(x, v) \tag{2.32}$$

has a solution. This solution satisfies $A'(x) = 0$, that is, $-2\text{div}\,(\nabla x) + 2v = 0$. Hence $v = \text{div}\,(\nabla x) \in G^d$, and we conclude that $X_0 \subset G^d$.

■

The discretized functional associated to (2.3) is given by:

$$F(u, v) = \begin{cases} J(u) + \frac{1}{2\lambda} \|f - u - v\|_X^2 & \text{if } v \in G_\mu^d \\ +\infty & \text{if } v \in X \backslash G_\mu^d \end{cases} \tag{2.33}$$

F being defined on $X \times X$:

$$F(u, v) = \begin{cases} \sum_{1 \leq i,j \leq N} \left(|(\nabla u)_{i,j}| + \frac{1}{2\lambda} |f_{i,j} - u_{i,j} - v_{i,j}|^2 \right) & \text{if } v \in G_\mu^d \\ +\infty & \text{if } v \in X \backslash G_\mu^d \end{cases} \tag{2.34}$$

Tproblem we want to solve is:

$$\inf_{(u,v)\in X\times X} F(u,v) \tag{2.35}$$

2.3 Total variation minimization as a projection

Presentation: Recently, a projection algorithm to minimize the total variation has been proposed in [3]. The problem is:

$$\inf_{u\in X}\left(J(u)+\frac{1}{2\lambda}\|f-u\|_X^2\right) \tag{2.36}$$

In [3], the following result is shown:

Proposition 2.3. *The solution of (2.36) is given by:*

$$u = f - P_{\lambda K}(f) \tag{2.37}$$

where P is the orthogonal projector on λK, and where K is the set:

$$\{\mathrm{div}\,(g)/g\in X, |g_{i,j}|\leq 1\ \forall i,j\} \tag{2.38}$$

Remark: It is easy to check that, if $\lambda > 0$:

$$\lambda K = G_\lambda^d \tag{2.39}$$

Hints: We give here some elements to prove (2.37) (we follow [3]). We will introduce some notations.

J defined by (1.1) is homogeneous of degree one (i.e. $J(\lambda u)=\lambda J(u)\ \forall u$ and $\lambda > 0$), it is then standard (see [5, 12, 6]) that the Legendre-Fenchel transform of J

$$J^*(v) = \sup\left((u,v)_X - J(u)\right) \tag{2.40}$$

is the indicator function of a closed convex set K:

$$J^*(v) = \chi_K(v) = \begin{cases} 0 & \text{if } v\in K \\ +\infty & \text{otherwise} \end{cases} \tag{2.41}$$

Moreover (since J convex and l.s.c.), $J^{**} = J$, hence:

$$J(u) = \sup_{v \in K} (u, v)_X \tag{2.42}$$

Now, if u is a minimizer of (2.36), then necessarily

$$0 \in \frac{u - f}{\lambda} + \partial J(u) \tag{2.43}$$

We denote by ∂H the subdifferential of H (see [12, 6]), and we recall that

$$w \in \partial H(u) \Longleftrightarrow H(v) \geq H(u) + (w, v - u)_X \text{ , for all } v \text{ in } X \tag{2.44}$$

(2.43) is equivalent to

$$\frac{f - u}{\lambda} \in \partial J(u) \tag{2.45}$$

Here, we switch to the dual formulation using a well–known identity in convex analysis (see corollary 5.2 in [5]), that asserts that (2.45) is equivalent to:

$$u \in \partial J^* \left(\frac{f - u}{\lambda} \right) \tag{2.46}$$

or

$$0 \in \frac{f - u}{\lambda} - \frac{f}{\lambda} + \frac{1}{\lambda} \partial J^* \left(\frac{f - u}{\lambda} \right) \tag{2.47}$$

so that we get that $w = \frac{f-u}{\lambda}$ is the minimizer of

$$\frac{\left\| w - \frac{f}{\lambda} \right\|^2}{2} + \frac{1}{\lambda} J^*(w). \tag{2.48}$$

Being J^* given by (2.41)), it yields that $w = \frac{f-u}{\lambda}$ is given by the orthogonal projection of $\frac{f}{\lambda}$ on the convex K.

We remark that

$$P_K \left(\frac{f}{\lambda} \right) = \frac{1}{\lambda} P_{\lambda K}(f) \tag{2.49}$$

then we deduce (2.37).

Algorithm: [3] gives an algorithm to compute $P_{\lambda K}(f)$. It indeed amounts to find:

$$\min\left\{\|\lambda \mathrm{div}\,(p) - f\|_X^2 : p \;/\; |p_{i,j}| \leq 1 \;\forall i,j = 1,\ldots,N\right\} \tag{2.50}$$

This problem can be solved by a fixed point method:

$$p^0 = 0 \tag{2.51}$$

and

$$p_{i,j}^{n+1} = \frac{p_{i,j}^n + \tau(\nabla(\mathrm{div}\,(p^n) - f/\lambda))_{i,j}}{1 + \tau|(\nabla(\mathrm{div}\,(p^n) - f/\lambda))_{i,j}|} \tag{2.52}$$

In [3] is given a sufficient condition ensuring the convergence of the algorithm:

Theorem 2.1. *Assume that the parameter τ in (2.52) verifies $\tau \leq 1/8$. Then $\lambda \mathrm{div}\,(p^n)$ converges to $P_{\lambda K}(f)$ as $n \to +\infty$.*

2.4 Application to our case

Since J^* is the indicator function of G_1^d (see (2.16) and (2.41)), we can rewrite (2.33) as

$$F(u,v) = \frac{1}{2\lambda}\|f - u - v\|_X^2 + J(u) + J^*\left(\frac{v}{\mu}\right) \tag{2.53}$$

With this formulation, we see clearly the symmetric roles played by u and v.

And the problem we want to solve is:

$$\inf_{(u,v)\in X\times X} F(u,v) \tag{2.54}$$

For solving (2.54), we consider the two following problems:

- v being fixed, we search for u as a solution of:

$$\inf_{u\in X}\left(J(u) + \frac{1}{2\lambda}\|f - u - v\|_X^2\right) \tag{2.55}$$

- u being fixed, we search for v as a solution of:

$$\inf_{v\in G_\mu^d} \|f - u - v\|_X^2 \tag{2.56}$$

From Proposition 2.3, we know that the solution of (2.55) is given by:

$$\hat{u} = f - v - P_{\lambda K}(f - v) \tag{2.57}$$

And as $G_\mu^d = \mu K$, the solution of (2.56) is simply given by:

$$\hat{v} = P_{\mu K}(f - u) \tag{2.58}$$

2.5 Algorithm

To solve problem (2.54), we consider both problems (2.55) and (2.56) successively.

1. Initialization:
$$u_0 = v_0 = 0 \tag{2.59}$$
2. Iterations:
$$v_{n+1} = P_{\mu K}(f - u_n) \tag{2.60}$$
$$u_{n+1} = f - v_{n+1} - P_{\lambda K}(f - v_{n+1}) \tag{2.61}$$
3. Stopping test: we stop if
$$\max(|u_{n+1} - u_n|, |v_{n+1} - v_n|) \leq \epsilon \tag{2.62}$$

2.6 Some comments about the algorithm

The choice of minimizing first with respect to v and then with respect to u plays an important role concerning the convergence speed of the algorithm. As we will see, the parameter λ has to be close to 0 for our problem to effectively be linked to Meyer's one. When we fix the parameters λ and μ, we choose them in particular such that $\lambda < \mu$ and even $\lambda << \mu$.

Let us consider the algorithm:

1. Initialization:
$$u_0 = v_0 = 0 \tag{2.63}$$

2. Iterations:

$$u_{n+1} = f - v_n - P_{\lambda K}(f - v_n) \tag{2.64}$$

$$v_{n+1} = P_{\mu K}(f - u_{n+1}) \tag{2.65}$$

3. Stopping test: we stop if

$$\max(|u_{n+1} - u_n|, |v_{n+1} - v_n|) \leq \epsilon \tag{2.66}$$

This algorithm is almost the same as the one we use; the difference is that we begin by minimizing with respect to u before minimizing with respect to v.

It is easy to show by induction that as long as $n \leq \mu/\lambda$ and $\|v_n\|_{G^d} \leq n\lambda$ then

Lemma 2.3. *Assume $(n+1)\lambda \leq \mu$ and $\|v_n\|_{G^d} \leq n\lambda$. Then we have:*

$$\|v_{n+1}\|_{G^d} \leq (n+1)\lambda \tag{2.67}$$

Proof: It suffices to notice that:

$$v_{n+1} = P_{\mu K}(f - u_{n+1}) = P_{\mu K}(v_n + P_{\lambda K}(f - v_n)) = v_n + P_{\lambda K}(f - v_n). \tag{2.68}$$

■

Assume that the solution we want to get is (u, v). In order that the solution of problem (2.54) corresponds to a discrete version of problem (1.3), we have to choose μ such that $\|v\|_{G^d} \leq \mu$ (we will precise this point in Section 3). So if $k\lambda \leq \|v\|_{G^d} < (k+1)\lambda$, we cannot expect the algorithm to converge before $k+1$ iterations (where an iteration corresponds to the passage from (u_n, v_n) to (u_{n+1}, v_{n+1})). Indeed, as $v_0 = 0$ we see from Lemma 2.3 that if $n \leq k$ then

$$\|v_n\|_{G^d} \leq n\lambda \leq k\lambda < \underbrace{\mu}_{=\|v\|_{G^d}} \tag{2.69}$$

And in the case when $\lambda << \|v\|_{G^d}$ (which is the case in practice), we then have $n >> 1$.

To avoid this lower bound for the time of convergence, we have chosen to minimize first with respect to v and then with respect to u in our algorithm. Experimentally, we have checked that our choice was indeed the faster.

3. Mathematical results

In this section we carry out the mathematical study of the algorithm (2.59)–(2.62). We first show its convergence when λ is fixed. We then precise the link of the limit of our model (when λ goes to 0) with Meyer'sone.

3.1 Study of F

Lemma 3.1. *There exists a unique couple $(\hat{u}, \hat{v}) \in X \times G_\mu^d$ minimizing F on $X \times X$.*

Proof: We split the proof into two steps.
Step 1: Existence

1. We first remark that the set $X \times G_\mu^d$ is convex, and then that F is convex on $X \times G_\mu^d$. We thus deduce that F is convex on $X \times X$.

2. It is immediate to see that F is continuous on $X \times G_\mu^d$. We then deduce that F is lower semi-continuous on $X \times X$.

3. Let $(u, v) \in X \times G_\mu^d$. We have

$$\|v\|_{G^d} \leq \mu \tag{3.1}$$

Moreover, since X is of finite dimension, there exists $g \in X$ such that $v = \mathrm{div}\,(g)$ and $\|g\|_{L^\infty} = \|v\|_{G^d} \leq \mu$. We deduce from (2.12) that (N^2 is the size of the image):

$$\|v\|_X =\leq 4\mu N^2 \tag{3.2}$$

We recall that $X \times X$ is endowed with the Euclidean norm (anyway, since $X \times X$ is of finite dimension, all the norms are equivalent)

$$\|(u, v)\|_{X\times X} = \sqrt{\|u\|_X^2 + \|v\|_X^2} \tag{3.3}$$

Thus, if

$$\|(u, v)\|_{X\times X} \to +\infty \tag{3.4}$$

then we get from (3.2) that $\|u\|_X \to +\infty$. We therefore deduce, since f is fixed, and since (3.2) holds, that

$$\|f-u-v\|_X^2 \to +\infty \tag{3.5}$$

And since $F(u,v) \geq \frac{1}{2\lambda}\|f-u-v\|_2^2$, we get

$$F(u,v) \to +\infty \tag{3.6}$$

We deduce that F is coercive on $X \times G_\mu^d$, hence on $X \times X$.

We deduce the existence of a minimizer $(\hat{u},\hat{v})$.

Step 2: Uniqueness
To get the uniqueness, we first remark that F is strictly convex on $X \times G_\mu^d$, as the sum of a convex function and of a strictly convex function, except in the direction $(u,-u)$. Hence it suffices to check that if $(\hat{u},\hat{v})$ is a minimizer of F then for $t \neq 0$, $(\hat{u}+t\hat{u},\hat{v}-t\hat{u})$ is not a minimizer of F. The result is obvious if $\hat{v}-t\hat{u} \in X \backslash G_\mu^d$. Let us show that if $\hat{v}-t\hat{u} \in G_\mu^d$ then the result is still true. Indeed, if $\hat{v}-t\hat{u} \in G_\mu^d$, we have:

$$F(\hat{u}+t\hat{u},\hat{v}-t\hat{u}) = F(\hat{u},\hat{v}) + (|1+t|-1)J(\hat{u}) \tag{3.7}$$

By contradiction, let us assume that there exists $\hat{t} \neq \{-2,0\}$ such that $\hat{v}-\hat{t}\hat{u} \in G_\mu^d$ and

$$F(\hat{u}+\hat{t}\hat{u},\hat{v}-\hat{t}\hat{u}) \leq F(\hat{u},\hat{v}) \tag{3.8}$$

As $(\hat{u},\hat{v})$ minimizes F, (3.8) is an equality. From (3.7), we deduce that $(|1+\hat{t}|-1)J(\hat{u}) = 0$. And as $\hat{t} \neq \{-2,0\}$, we get that $J(\hat{u}) = 0$. There exists therefore $\gamma \in \mathbb{R}$ such that for all (i,j), $\hat{u}_{i,j} = \gamma$.

1. If $\gamma = 0$, then $\hat{u} = 0$. Thus $(\hat{u}+\hat{t}\hat{u},\hat{v}-\hat{t}\hat{u}) = (\hat{u},\hat{v})$.
2. If $\gamma \neq 0$, then $\hat{v}-\hat{t}\hat{u}$ cannot belong to G_μ^d since its mean is not 0 (see Proposition 2.2). This contradicts our assumption.

There remains to check what happens in the case when $\hat{t} = -2$. In this case, we have: $F(-\hat{u},\hat{v}+2\hat{u}) \leq F(\hat{u},\hat{v})$, i.e. $(-\hat{u},\hat{v}+2\hat{u})$ is also a minimizer of F. As we assume $\hat{v}+2\hat{u} \in G_\mu^d$, and as F convex (and as G_μ^d convex), we get:

$$F(0,\hat{u}+\hat{v}) \leq \frac{1}{2}F(\hat{u},\hat{v}) + \frac{1}{2}F(-\hat{u},\hat{v}+2\hat{u}) \tag{3.9}$$

And we deduce that $(0, \hat{u}+\hat{v})$ is also a minimizer of F. But $F(0, \hat{u}+\hat{v}) = F(\hat{u}, \hat{v})$, i.e. $\frac{1}{2\lambda}\|f-\hat{u}-\hat{v}\|_X^2 = J(\hat{u}) + \frac{1}{2\lambda}\|f-\hat{u}-\hat{v}\|_X^2$. We thus get that $J(\hat{u}) = 0$, and we conclude as before.

Hence there exists a unique couple $(\hat{u}, \hat{v}) \in X \times G_\mu^d$ minimizing F on $X \times X$.

■

3.2 Convergence of the algorithm

We show here that our algorithm gives asymtotically the solution of the discrete problem associated to (2.54).

Proposition 3.1. *The sequence $F(u_n, v_n)$ built in Section 2.5 converges to the minimum of F on $X \times X$.*

Proof: We first remark that, as we solve successive minimization problems, we have:

$$F(u_n, v_n) \geq F(u_n, v_{n+1}) \geq F(u_{n+1}, v_{n+1}) \tag{3.10}$$

In particular, the sequence $F(u_n, v_n)$ is nonincreasing. As it is bounded from below by 0, it thus converges in $\mathbb{R}$. We denote by m its limit. We want to show that

$$m = \inf_{(u,v)\in X\times X} F(u, v) \tag{3.11}$$

Without any restriction, we can assume that, $\forall n$, $(u_n, v_n) \in X \times G_\mu^d$.

As F is coercive and as the sequence $F(u_n, v_n)$ converges, we deduce that the sequence (u_n, v_n) is bounded in $X \times G_\mu^d$.

We can thus extract a subsequence (u_{n_k}, v_{n_k}) which converges to $(\hat{u}, \hat{v})$ as $n_k \to +\infty$, with $(\hat{u}, \hat{v}) \in X \times G_\mu^d$.

Moreover, we have, for all $n_k \in \mathbb{N}$ and all v in X:

$$F(u_{n_k}, v_{n_k+1}) \leq F(u_{n_k}, v) \tag{3.12}$$

and for all $n_k \in \mathbb{N}$ and all u in X:

$$F(u_{n_k}, v_{n_k}) \leq F(u, v_{n_k}) \tag{3.13}$$

Let us denote by $\bar{v}$ a cluster point of (v_{n_k+1}). Considering (3.10), we get (since F is continuous on $X \times G_\mu^d$):

$$m = F(\hat{u}, \hat{v}) = F(\hat{u}, \bar{v}) \tag{3.14}$$

By passing to the limit in (2.60), we get:

$$\bar{v} = P_{\mu K}(f - \hat{u}) \tag{3.15}$$

But from (3.14), we know that:

$$\|f - \hat{u} - \hat{v}\| = \|f - \hat{u} - \bar{v}\| \tag{3.16}$$

By uniqueness of the projection, we conclude that $\bar{v} = \hat{v}$. Hence $v_{n_k+1} \to \hat{v}$.

By passing to the limit in (3.12) (F is continuous on $X \times G_\mu^d$), we therefore have for all v:

$$F(\hat{u}, \hat{v}) \leq F(\hat{u}, v) \tag{3.17}$$

And by passing to the limit in (3.13), for all u:

$$F(\hat{u}, \hat{v}) \leq F(u, \hat{v}) \tag{3.18}$$

(3.17) can be rewritten:

$$F(\hat{u}, \hat{v}) = \inf_{v \in X} F(\hat{u}, v) \tag{3.19}$$

and (3.18):

$$F(\hat{u}, \hat{v}) = \inf_{u \in X} F(u, \hat{v}) \tag{3.20}$$

But, from the definition of $F(u, v)$ (see (2.53)), (3.20) is equivalent to (see [12, 6]):

$$0 \in -f + \hat{u} + \hat{v} + \lambda \partial J(\hat{u}) \tag{3.21}$$

and (3.19) to:

$$0 \in -f + \hat{u} + \hat{v} + \lambda \partial J^* \left(\frac{\hat{v}}{\mu} \right) \tag{3.22}$$

But the subdifferential of F at $(\hat{u},\hat{v})$ is given by

$$\partial F(\hat{u},\hat{v}) = \partial\left(\frac{1}{2\lambda}\|f-\hat{u}-\hat{v}\|_X^2 + J(\hat{u}) + J^*\left(\frac{\hat{v}}{\mu}\right)\right) \quad (3.23)$$

$$= \partial\left(\frac{1}{2\lambda}\|f-\hat{u}-\hat{v}\|_X^2\right) + \partial\left(J(\hat{u}) + J^*\left(\frac{\hat{v}}{\mu}\right)\right) \quad (3.24)$$

As $\|f-\hat{u}-\hat{v}\|_X^2$ differentiable at $(\hat{u},\hat{v})$, we even have:

$$\partial\left(\frac{1}{2\lambda}\|f-\hat{u}-\hat{v}\|_X^2\right) = \left\{\frac{1}{\lambda}\begin{pmatrix} -f+\hat{u}+\hat{v} \\ -f+\hat{u}+\hat{v}\end{pmatrix}\right\} \quad (3.25)$$

And (since J is continuous):

$$\partial\left(J(\hat{u}) + J^*\left(\frac{\hat{v}}{\mu}\right)\right) = \begin{pmatrix} \partial J(\hat{u}) \\ \partial J^*\left(\frac{\hat{v}}{\mu}\right)\end{pmatrix} \quad (3.26)$$

Hence:

$$\partial F(\hat{u},\hat{v}) = \frac{1}{\lambda}\begin{pmatrix} -f+\hat{u}+\hat{v}+\lambda\partial J(\hat{u}) \\ -f+\hat{u}+\hat{v}+\lambda\partial J^*\left(\frac{\hat{v}}{\mu}\right)\end{pmatrix} \quad (3.27)$$

And thus, according to (3.21) and (3.22), we have:

$$\left\{\begin{pmatrix} 0 \\ 0\end{pmatrix}\right\} \in \partial F(\hat{u},\hat{v}) \quad (3.28)$$

which is equivalent to:

$$F(\hat{u},\hat{v}) = \inf_{(u,v)\in X^2} F(u,v) = m \quad (3.29)$$

Hence the whole sequence $F(u_n,v_n)$ converges towards m the unique minimum of F on $X\times G_\mu^d$. We deduce that the sequence (u_n,v_n) converges to $(\hat{u},\hat{v})$, the minimizer of F, when n tends to $+\infty$.

■

Remarks:

1. It is to be noticed that theorem 2.1 still holds for the minimization of F with respect to v (resp. u) when u (resp. v) is fixed.

2. It is not true in general that, for F strictly convex, the two following properties
$$F(\hat{u},\hat{v}) \leq F(\hat{u},v)\ \forall v$$
$$F(\hat{u},\hat{v}) \leq F(u,\hat{v})\ \forall u$$
imply
$$F(\hat{u},\hat{v}) \leq F(u,v)\ \forall u,v$$
Indeed, [6] gives a counter-example with the function:
$$F(u,v) = |u-v| + \frac{1}{2}(u+1)^2 + \frac{1}{2}(v+1)^2 \tag{3.30}$$
It is immediate to check that $(-1,-1)$ is the minimizer of F, and that $(0,0)$ is a minimizer of both $u \mapsto F(u,0)$ and $v \mapsto F(0,v)$.

We end this subsection with the following result:

Proposition 3.2. *The assertion*
$$F(\hat{u},\hat{v}) = \inf_{(u,v)\in X\times X} F(u,v) \tag{3.31}$$
is equivalent to
$$\begin{cases} \hat{u} = f - \hat{v} - P_{\lambda K}(f-\hat{v}) \\ \hat{v} = P_{\mu K}(f-\hat{u}) \end{cases} \tag{3.32}$$

Proof: The proof is a consequence of Propositions 2.3 and 3.1.

■

Remark: Proposition 3.2 shows that our algorithm relies on a fixed point result for both u and v.

3.3 Link with Meyer's model

We examine here the link between the discrete model (2.54) and Meyer's problem.

We first recall the discrete version of Meyer's problem:

$$\inf_{(u,v)\in X\times G^d / f=u+v} H_\alpha(u,v) \tag{3.33}$$

with

$$H_\alpha(u,v) = (J(u) + \alpha\|v\|_{G^d}) \tag{3.34}$$

Lemma 3.2. *There exists a solution $(\hat{u},\hat{v}) \in X \times G^d$ of problem (3.33).*

Proof: (3.33) is equivalent to

$$\inf_{v\in G^d} H_\alpha(f-v,v) \tag{3.35}$$

It is immediate to verify that H_α is convex, coercive and continuous on G^d. Hence there exists $\hat{v} \in G^d$ such that

$$H_\alpha(f-\hat{v},\hat{v}) = \inf_{v\in G^d} H_\alpha(f-v,v) \tag{3.36}$$

Let us denote $\hat{u} = f - \hat{v}$. Then $(\hat{u},\hat{v})$ is a solution of (3.33).

■

Remark: We do not know if a uniqueness result holds for problem (3.33).

We then recall problem (2.54):

$$\inf_{(u,v)\in X\times X} F_{\lambda,\mu}(u,v) \tag{3.37}$$

with

$$F_{\lambda,\mu}(u,v) = \frac{1}{2\lambda}\|f-u-v\|^2 + J(u) + J^*\left(\frac{v}{\mu}\right) \tag{3.38}$$

Let us consider the problem

$$\inf_{(u,v)\in X\times X/f=u+v} J(u) + J^*\left(\frac{v}{\mu}\right) \tag{3.39}$$

Lemma 3.3. *There exists $(\bar{u},\bar{v}) \in X \times X$ solution of (3.39).*

Proof: (3.39) is equivalent to

$$\inf_{v\in X} J(f-v) + J^*\left(\frac{v}{\mu}\right) \tag{3.40}$$

It is immediate to see that the function to minimize in (3.40) is convex, coercive and lower semi-continuous on X. Hence there exists $\bar{v} \in X$ such that

$$J(f-\bar{v}) + J^*\left(\frac{\bar{v}}{\mu}\right) = \inf_{v\in X} J(f-v) + J^*\left(\frac{v}{\mu}\right) \tag{3.41}$$

Denoting by $\bar{u} = f - \bar{v}$. Then $(\bar{u},\bar{v})$ is a solution of (3.39).

■

Remark: It is clear that the set S of solutions of problem (3.39) is a closed convex set.

Proposition 3.4 below will show the link between (3.37) and (3.39).

Proposition 3.3. *Let us fix $\alpha > 0$ in problem (3.33). Let $(\hat{u},\hat{v})$ a solution of problem (3.33). Then:*

- *$(\hat{u},\hat{v})$ is also a solution of problem (3.39).*
- *Conversely, any solution $(\bar{u},\bar{v})$ of (3.39) (with $\mu = \|\hat{v}\|_{G^d}$) is a solution of (3.33).*

Proof: We split the proof into two steps.
Step 1:
We first want to show that $(\hat{u},\hat{v})$ is a solution of (3.39) (with $\mu = \|\hat{v}\|_{G^d}$. As $(\hat{u},\hat{v})$ is a solution of (3.33) (the existence of $(\hat{u},\hat{v})$ is given by Lemma 3.2) and as $\|\hat{v}\|_{G^d} = \mu$, then $\hat{u}$ is solution of

$$\inf_{u\in X/u=f-v,\|v\|_{G^d}=\mu} J(u) \tag{3.42}$$

Since $\{u \in X/u = f - v, \|v\|_{G^d} = \mu\}$ is contained in $\{u \in X/u = f - v, \|v\|_{G^d} \leq \mu\}$, we have:

$$\inf_{u\in X/u=f-v,\|v\|_{G^d}=\mu} J(u) \geq \inf_{u\in X/u=f-v,\|v\|_{G^d}\leq\mu} J(u) \tag{3.43}$$

By contradiction, let us assume that

$$\inf_{u\in X/u=f-v,\|v\|_{G^d}=\mu} J(u) > \inf_{u\in X/u=f-v,\|v\|_{G^d}\leq\mu} J(u) \tag{3.44}$$

Thus, there exists $v' \in X$ such that $\|v'\|_{G^d} < \mu$ and

$$J(f - v') < \inf_{u\in X/u=f-v,\|v\|_{G^d}=\mu} J(u) \tag{3.45}$$

Denoting by $u' = f - v'$, we have:

$$J(u') + \alpha\|v'\|_{G^d} < J(u') + \alpha\mu \tag{3.46}$$

But since $(\hat{u},\hat{v})$ is a solution of (3.33):

$$J(\hat{u}) + \alpha\|\hat{v}\|_{G^d} \leq J(u') + \alpha\|v'\|_{G^d} < J(u') + \alpha\mu \tag{3.47}$$

Hence (we recall that $\|\hat{v}\|_{G^d} = \mu$), we get from (3.47) that

$$J(\hat{u}) < J(u') \tag{3.48}$$

This contradicts (3.45).

We conclude that (3.44) cannot hold. Hence:

$$\inf_{u\in X/u=f-v,\|v\|_{G^d}=\mu} J(u) = \inf_{u\in X/u=f-v,\|v\|_{G^d}\leq\mu} J(u) \tag{3.49}$$

From (3.42), we see that $\hat{u}$ is solution of

$$\inf_{u \in X / u = f - v, \|v\|_{G^d} \leq \mu} J(u) \tag{3.50}$$

i.e. $\hat{u}$ is solution of

$$\inf_{u \in X / u = f - v} J(u) + J^* \left(\frac{v}{\mu} \right) \tag{3.51}$$

Hence $(\hat{u}, \hat{v})$ is also a solution of (3.39).
Step 2:
Let us now consider $(\bar{u}, \bar{v})$ a solution of (3.39) (the existence of $(\bar{u}, \bar{v})$ is given by Lemma 3.3). We can repeat the computations we made in Step 1. We get that $\bar{u}$ is a solution of:

$$\inf_{u \in X / u = f - v, \|v\|_{G^d} = \mu} J(u) + \alpha \mu \tag{3.52}$$

We therefore have:

$$J(\bar{u}) + \alpha \mu = J(\hat{u}) + \alpha \|\hat{v}\|_{G^d} \tag{3.53}$$

But as $(\bar{u}, \bar{v})$ is a solution of (3.39), we have

$$\|\bar{v}\|_{G^d} \leq \mu \tag{3.54}$$

Hence

$$J(\bar{u}) + \alpha \|\bar{v}\|_{G^d} \leq J(\hat{u}) + \alpha \|\hat{v}\|_{G^d} \tag{3.55}$$

And since $(\hat{u}, \hat{v})$ is a solution of (3.33), we get that:

$$J(\bar{u}) + \alpha \|\bar{v}\|_{G^d} = J(\hat{u}) + \alpha \|\hat{v}\|_{G^d} \tag{3.56}$$

We thus conclude that $(\bar{u}, \bar{v})$ is a solution of (3.33).

■

3.4 Role of λ

We show here that problem (3.39) is obtained by passing to the limit $\lambda \to 0^+$ in (3.37).

Proposition 3.4. *Let us fix $\alpha > 0$ in (3.33). Let us assume that problem (3.33) has a unique solution $(\hat{u}, \hat{v})$. Set $\mu = \|\hat{v}\|_{G^d}$ in (3.37) and (3.39). Let us denote (u_λ, v_λ) the solution of problem (3.37). Then (u_λ, v_λ) converges to $(u_0, v_0) \in X \times X$ as λ goes to 0. Moreover, $(u_0, v_0) = (\hat{u}, \hat{v})$ is the solution of problem (3.39).*

Remark: In the case when the solution of problem (3.33) is not unique, the result of Proposition 3.4 does not hold. We can just show that any cluster point of $(u_{\lambda_n}, v_{\lambda_n})$ is a solution of problem (3.39) and thus of (3.33) (and we know that the set S of the solutions of problem (3.39) is a closed convex set).

$\forall \epsilon > 0$, there exists $\Lambda > 0$ such that $\forall \lambda \in]0; \Lambda[$,

$$(u_\lambda, v_\lambda) \in S_\epsilon \tag{3.57}$$

where

$$S_\epsilon = \{x \in X \ / \ \exists s \in S \text{ such that } \|x - s\| \leq \epsilon\} \tag{3.58}$$

Proof of Proposition 3.4: The existence of $(\hat{u}, \hat{v})$ is given by Lemma 3.3. The existence and uniqueness of (u_λ, v_λ) is given by Lemma 3.1.

Since (u_λ, v_λ) is the solution of problem (3.37), we have $v_\lambda \in G^d_\mu$, i.e.

$$\|v_\lambda\|_{G^d} \leq \mu \tag{3.59}$$

As we saw in the proof of Lemma 3.1, this inequality implies:

$$\|v_\lambda\|_X \leq 4\mu N^2 \tag{3.60}$$

Since (u_λ, v_λ) is the solution of problem (3.37), we have:

$$F_{\lambda,\mu}(u_\lambda, v_\lambda) \leq F_{\lambda,\mu}(f, 0) \tag{3.61}$$

which means

$$F_{\lambda,\mu}(u_\lambda, v_\lambda) \leq J(f) \tag{3.62}$$

And the left hand-side of (3.62) is given by:

$$F_{\lambda,\mu}(u_\lambda, v_\lambda) = J(u_\lambda) + \frac{1}{2\lambda}\|f - u_\lambda - v_\lambda\|_X^2 + J^*\left(\frac{v_\lambda}{\mu}\right) = J(u_\lambda) + \frac{1}{2\lambda}\|f - u_\lambda - v_\lambda\|_X^2 \tag{3.63}$$

Hence

$$J(u_\lambda) + \frac{1}{2\lambda}\|f - u_\lambda - v_\lambda\|_X^2 \leq J(f) \tag{3.64}$$

and

$$\|f - u_\lambda - v_\lambda\|^2 \leq 2\lambda J(f) \tag{3.65}$$

As $\|v_\lambda\|_X$ is bounded (from (3.60)), we conclude that if $\lambda \in [0; 1]$, u_λ is bounded by a constant $C > 0$ which does not depend on λ.

Consider a sequence (λ_n) which goes to 0 as $n \to +\infty$. Then, up to an extraction (since $(u_{\lambda_n}, v_{\lambda_n})$ is bounded in $X \times X$), there exists $(u_0, v_0) \in X \times X$ such that $(u_{\lambda_n}, v_{\lambda_n})$ converges to (u_0, v_0).

By passing to the limit in (3.65), we get:

$$\|f - u_0 - v_0\|_X = 0 \tag{3.66}$$

i.e.

$$f = u_0 + v_0 \tag{3.67}$$

To conclude the proof of the proposition, there remains to show that (u_0, v_0) is a solution of problem (3.39). We first notice that as $\forall \lambda > 0$, and since $\|v_\lambda\|_{G^d} \leq \mu$, we get

$$\|v_0\|_{G^d} \leq \mu \tag{3.68}$$

Let $(u, v) \in X \times X$ such that $f = u + v$. We have:

$$\begin{aligned}
& J(u) + J^*\left(\frac{v}{\mu}\right) + \frac{1}{2\lambda}\underbrace{\|f - u - v\|^2}_{=0} \\
\geq\ & J(u_{\lambda_n}) + J^*\left(\frac{v_{\lambda_n}}{\mu}\right) + \frac{1}{2\lambda_n}\|f - u_{\lambda_n} - v_{\lambda_n}\|^2 \\
\geq\ & \underbrace{J(u_{\lambda_n}) + J^*\left(\frac{v_{\lambda_n}}{\mu}\right)}_{\to J(u_0) + J^*\left(\frac{v_0}{\mu}\right)}
\end{aligned}$$

Hence (u_0, v_0) is a solution of problem (3.39). And as we have assumed that problem (3.39) has a unique solution, we deduce that $(u_0, v_0) = (\hat{u}, \hat{v})$, i.e. (u_0, v_0) is the solution of problem (3.39).

■

4. Comparison of our model with the total variational minimization

4.1 Introduction

In this section, we intend to compare Rudin-Osher-Fatemi (ROF) problem (1.2) with Meyer's one (1.3). We put some noise on an image furnished by the GdR-PRC ISIS (see Figure 1), and we perform both a total variation algorithm and our algorithm (2.59)–(2.62). We have chosen to use Chambolle's algorithm to minimize the total variation (see Subsection 2.3).

We display the results on Figures 2, 3 and 4. The "difference image" is obtained from the v components of both algorithms. We denote by v_{Meyer} the v component given by our algorithm, and v_{ROF} the one given by the total variation minimization algorithm. The value of a pixel in position (i, j) is 255.0 (i.e. white) if $v_{Meyer}(i, j) > v_{ROF}(i, j)$, 127.0 (i.e. gray) if $v_{Meyer}(i, j) = v_{ROF}(i, j)$, and 0.0 (i.e. black) if $v_{Meyer}(i, j) < v_{ROF}(i, j)$.

We add a gaussian noise of variance σ to the original image.

4.2 Commentaries

We compare the v component given by our algorithm with the one given by the total variation minimization algorithm. Their mean values are both very close to zero. For instance, in the case of Figure 3 ($\sigma = 50$), v_{Meyer} and v_{ROF} have almost the same mean value: -0.7.

In the case of the ROF problem, the parameter λ corresponds to the one in (1.2), and in the case of Meyer' problem, the parameters λ and μ correspond to the ones in (2.1). For a given noisy image, we tune these parameters so that $\|v_{Meyer}\|_{L^2} \simeq \|v_{ROF}\|_{L^2}$: the v components both contain the same quantity of information. We want to compare the information they contain.

Figure 1: Original synthetic image

One sees on the "difference image" that $v_{Meyer}(i,j) > v_{ROF}(i,j)$ in the darkest regions of the original image (figure 1), and that $v_{Meyer}(i,j) < v_{ROF}(i,j)$ in the lightest regions. This means that the v component in the ROF model depends more on the mean gray level value of the original image than in the case of Meyer's one.

For instance, let us have a look at the dark circle on top left of Figure 1. In the case of Figure 3 ($\sigma = 50$), the mean value of the pixels corresponding to this circle is -1.0 in v_{Meyer} and -4.2 in v_{ROF}. Both components v tend to have a negative mean because in Figure 1 the circle is a dark component.

In homogeneous regions (such as the dark circle we considered just before), we would expect the v component of both models to have a zero mean (the mean of the white gaussian noise we add to the original image). According to the remarks we made before, Meyer's model appears to loose less information than the ROF model.This confirms the assertions by Y. Meyer in [9]. The decomposition he proposes seems to be more adapted to image restoration. Nevertheless, the difference between both methods appears not to be visually very important.

We get the same kind of results with the Lenna image (see figure 5 and 6).

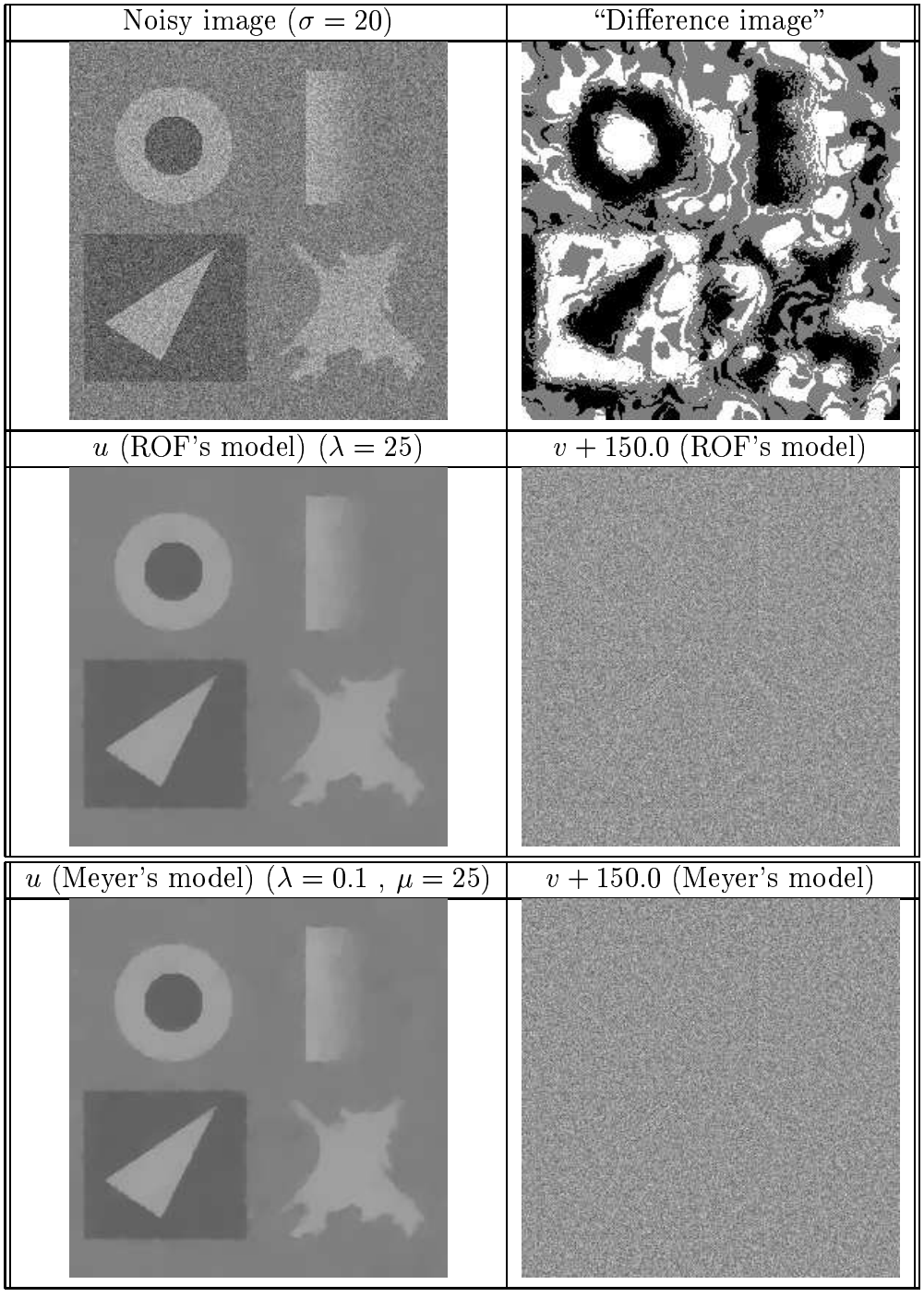

Figure 2: Comparison for $\sigma = 20$ (SNR=16.3)

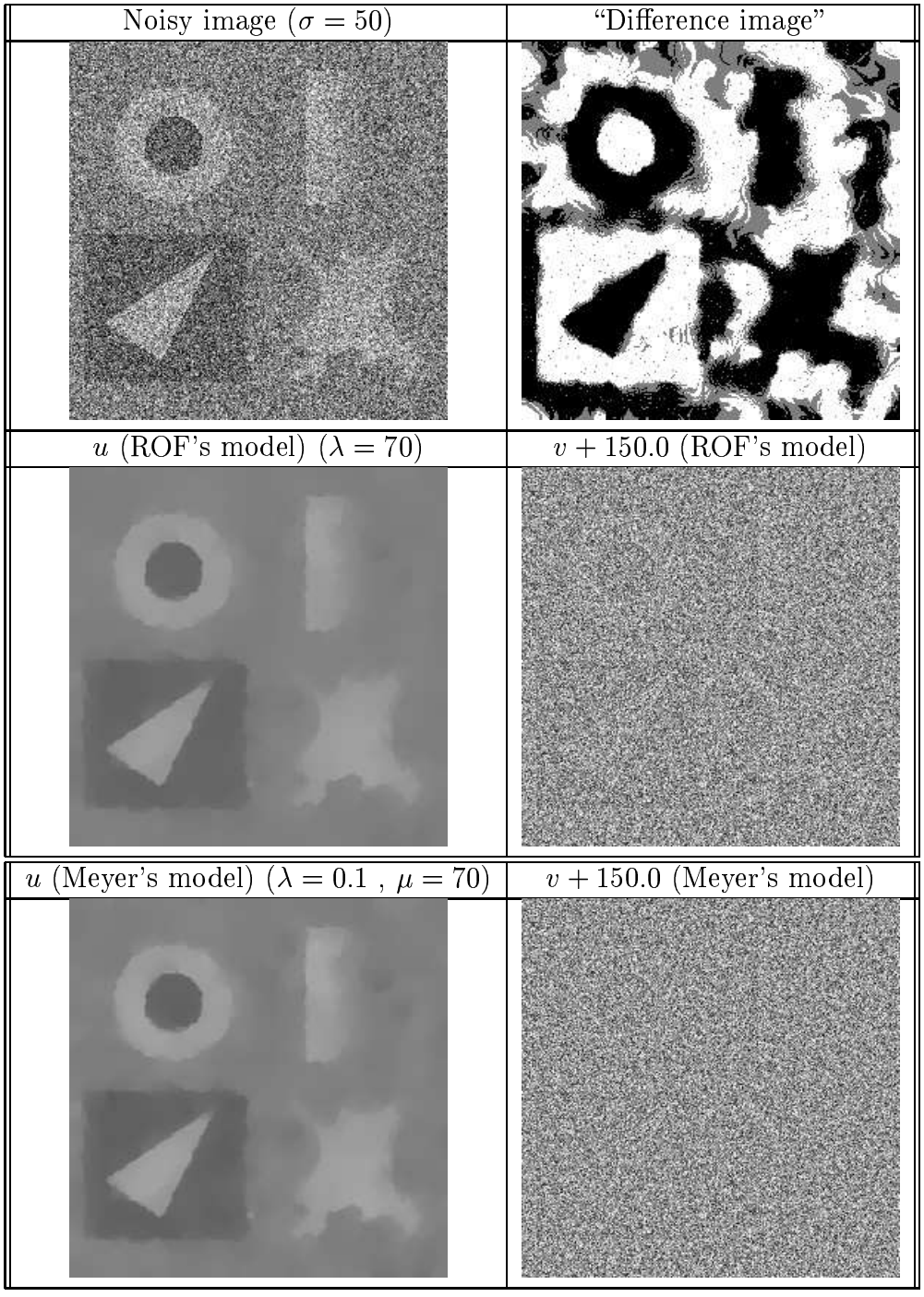

Figure 3: Comparison for $\sigma = 50$ (SNR=8.36)

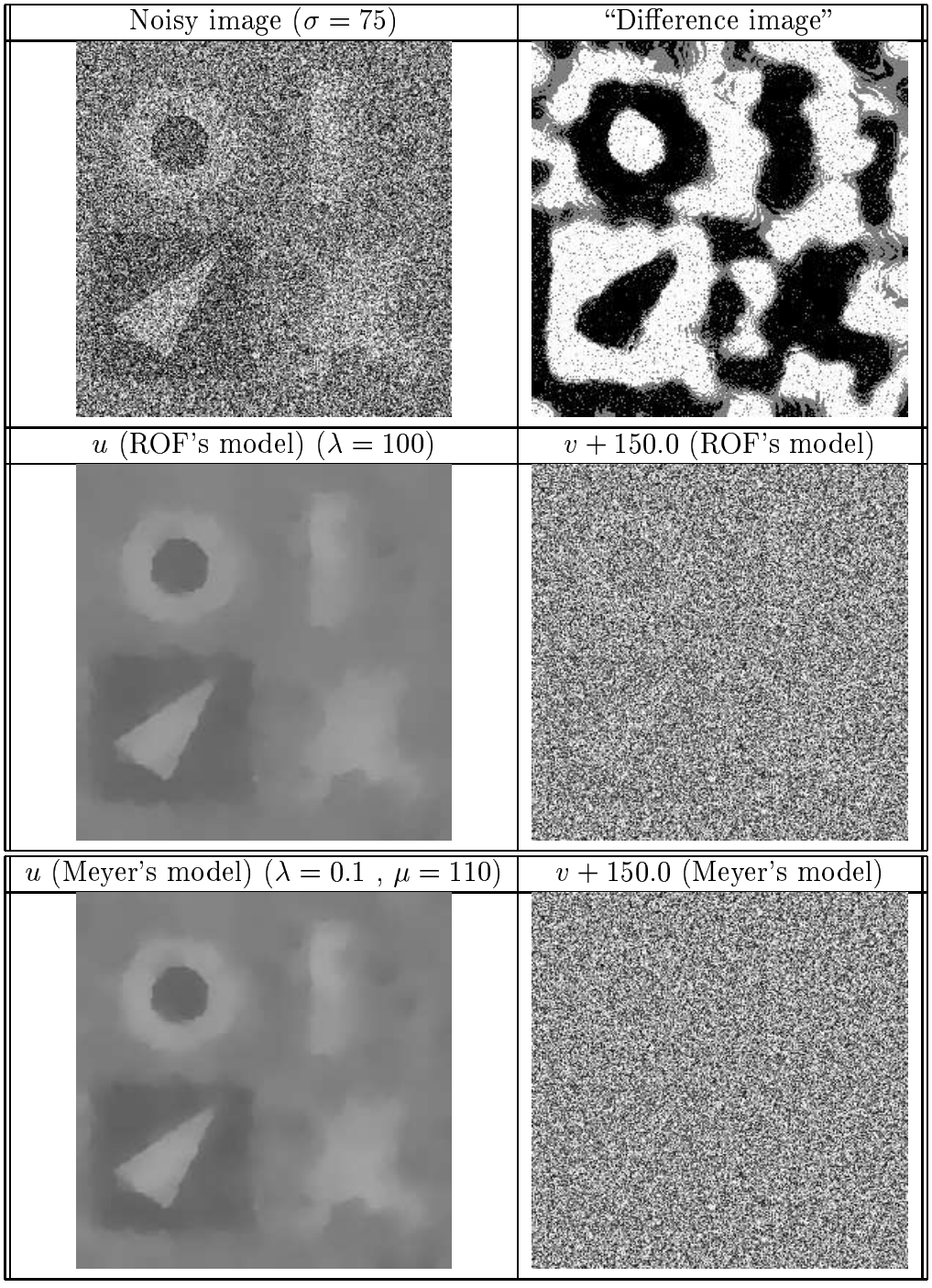

Figure 4: Comparison for $\sigma = 75$ (SNR=4.84)

Figure 5: Lenna image

5. Classification of textured images

5.1 Introduction

In this section, we show how the v component of a textured image f can be used to carry out classification on f. Indeed, thanks to lemma 1.1, we know that the v component is a signal with large oscillations. In particular, this component contains the textures of the original image f. When f is a non noisy image, v contains only the textures of f.

To classify the image, we use the model introduce by the three first authors in [2]. This model is based on a variational approach. It performs the supervised classification of a textured image. In this work, a functional specific to textures is proposed, textures being characterized through their energies in the different sub-bands of a wavelet packet decomposition. The Euler-Lagrange equations associated to this functional are embedded in a dynamical scheme whose steady state corresponds to the classification of the image.

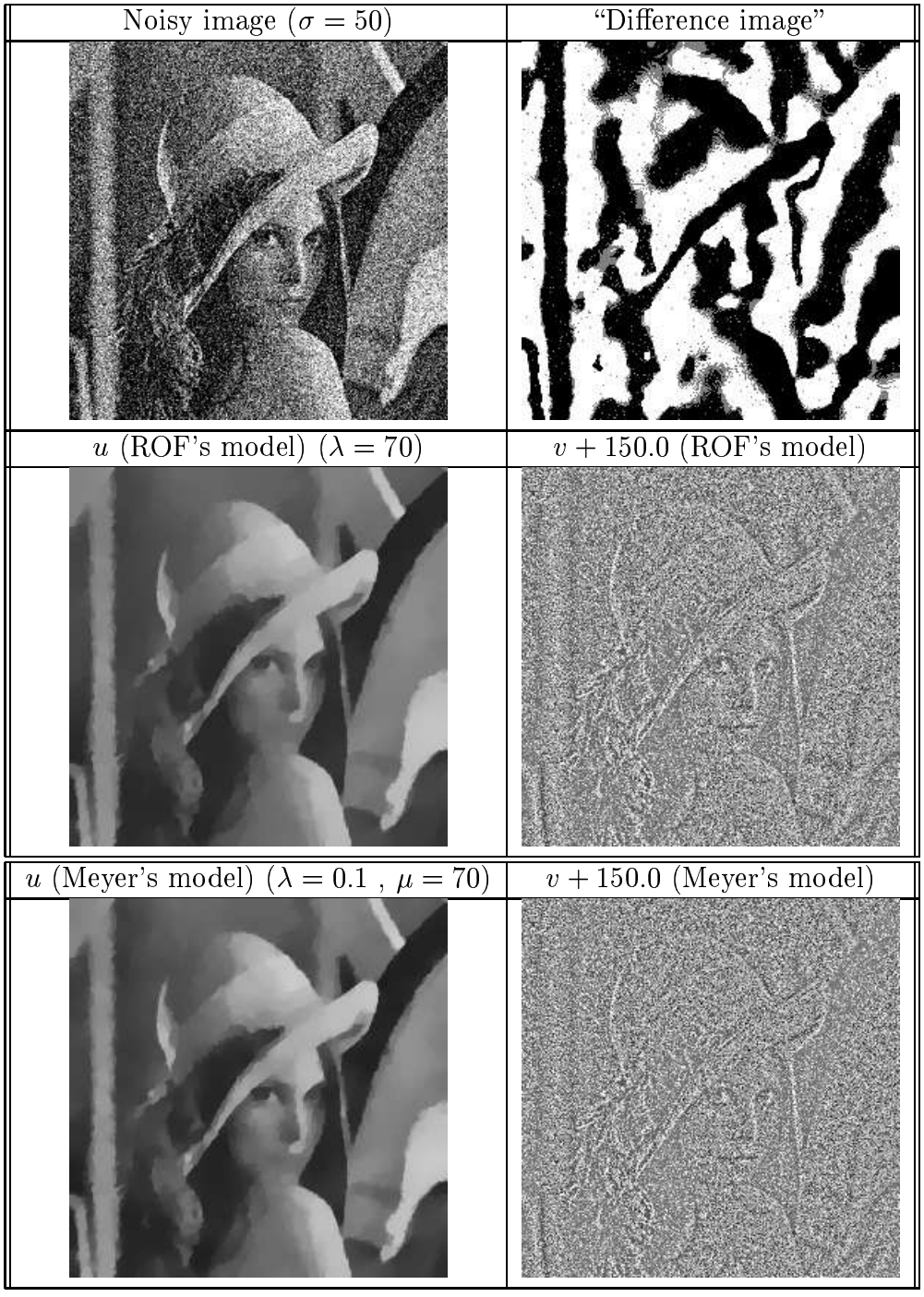

Figure 6: Comparison for $\sigma = 50$ (Lenna image). SNR=7.05

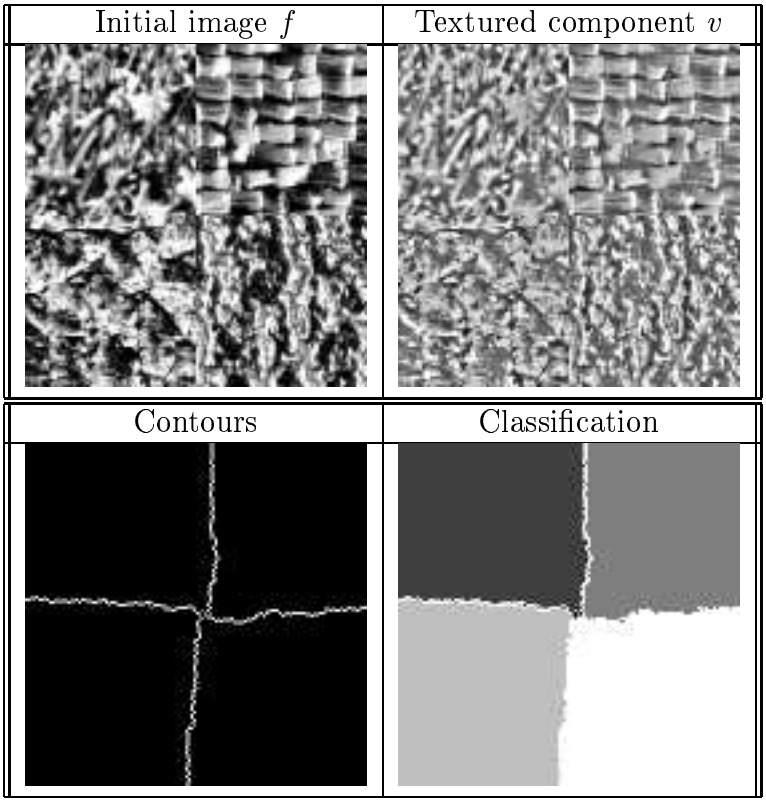

Figure 7: Example of classification on a synthetic image with four textures

5.2 Numerical results

The classification of the images are obtained on two steps. We begin by performing the decomposition of the image f into its two components u and v. Then we use the classification algorithm (see [2]) on v.

We present results on synthetic images in Figures 7 and 8. We give the initial image f, its v component, and the result of the obtained classification (from a contour point of view and from a set point of view).

The results we get here are comparable with the one we show in [2]. This confirms the fact that in Meyer's model, when the original image has no noise, than the v component contains the texture information of the original image.

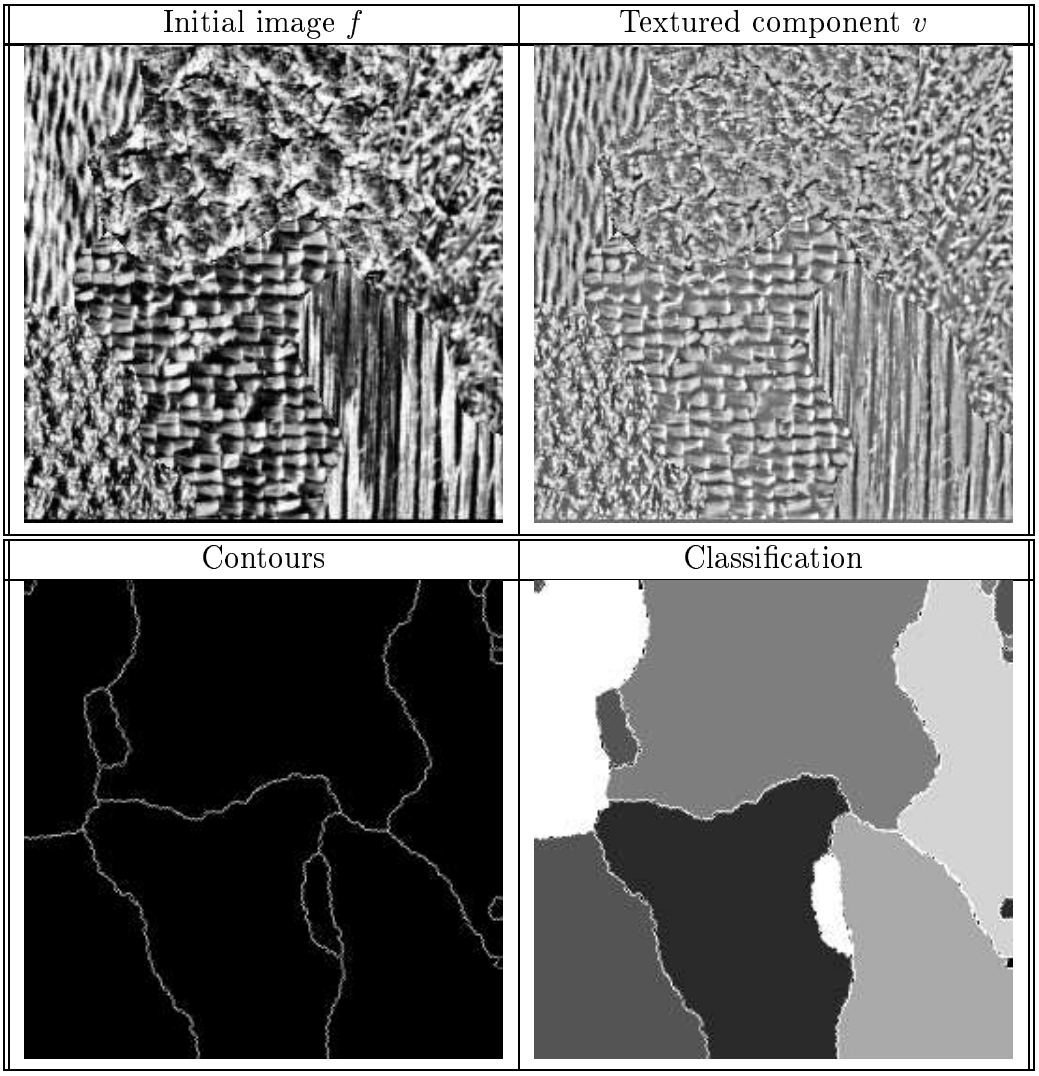

Figure 8: Example of classification on a synthetic image with six textures

6. SAR images restoration

6.1 Introduction

Synthetic Aperture Radar (SAR) images are strongly corrupted by a noise called speckle.

A radar sends a coherent wave, and get an image from the reflected wave it receives back [8, 7].

When one cares with the reflection of a coherent wave on a coarse surface, then one can see that the observed image is degraded by a noise of large amplitude. This gives a speckled aspect to the image. That is why such a noise is called speckle.

Difficulty of the problem: To illustrate oscillations that are present in radar images, we have cut slices in SAR images furnished by the CNES (see Figure 9).

Multiplicative noise: A classical way to study a SAR image consists in doing a multiplicative modelisation of the image [15, 10, 16], by I=RS, where I is the observed intensity, R the scene reflectivity, and S the speckle.

By using the notation of the previous sections, this amounts to decompose the image f into $f = uv$.

Link with our approach: In our model, the noise is considered to be additive: the image f is decomposed into a component u belonging to BV, and a component v in G. But it is to be noticed that our model is completely different from the classical additive models: in these ones, v is often considered to be a Gaussian white noise, and therefore has a constant variance all over the image. Here, v belongs to G, a space in which signals can have large oscillations but small norm. As recalled in lemma 1.1, a signal v in G may have a large norm (L^q , $q > 2$), and nevertheless its norm in G can be very small. Moreover the variance of the oscillations of v may not be uniform on the whole image. Remark that by considering u as the restored image (without speckle) we assume that there is no texture in the SAR image.

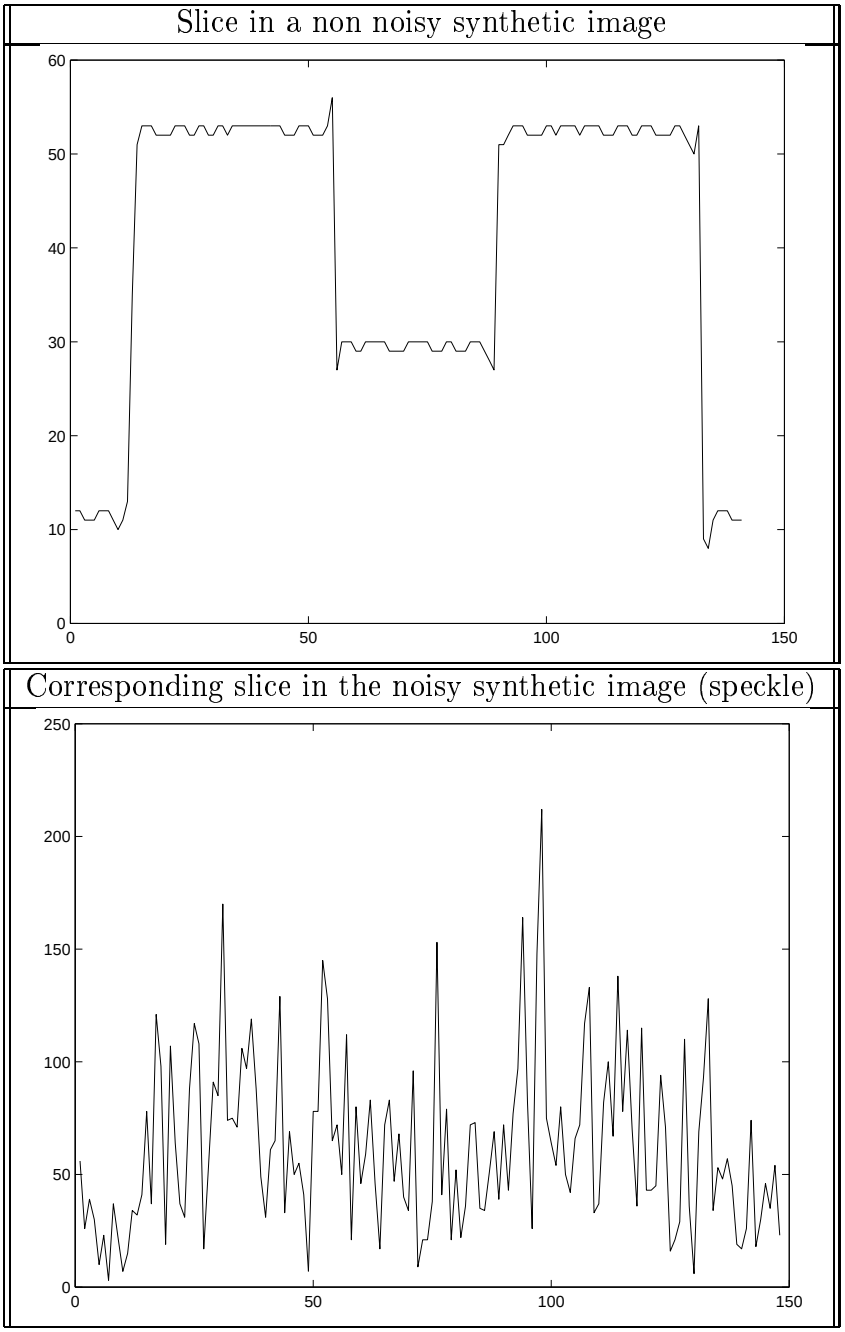

Figure 9: Speckle on a 1-D signal

6.2 Results on synthetic images

Restoration Figures 10, 11 and 12 show why for a SAR image the decomposition proposed by Meyer is very interesting. Indeed, one checks that the v component contains the speckle, and the u component can be regarded as a restoration of the original image (if it does not contain textures).

It is difficult to make comparisons with other methods, since the main criterion remains the visual interpretation. Nevertheless, the results we get appear good with respect to existing methods. And above all, our approach being a variational one, computation time are very short. With a processor at 800 MHz and 128 kilo of RAM, it takes less than one minute to deal with an image of size 256*256.

Classification We present each time a supervised classification result. Depending on the image we use two kinds of classification algorithms.

1. The first one is simply a thresholding algorithm. In the case of Figure 10, it gives a quasi-perfect classification of the image. But in the case of Figure 12, we see that we need to regularize the classes we get.

2. That is why we also use an algorithm introduced in [14]. This algorithm had been developed to carry out supervised classification of optical images. Each class is characterized by its gray level mean, as well as its variance, and follows a Gaussian distribution. Such a model is particularly well suited to classify the BV components u that we get from our decomposition algorithm. We can check it on Figure 12.

6.3 Results on real images

We use SAR images of Bourges' area provided by the CNES. The reference image (also furnished by the CNES) has been obtained by amplitude summation (this is the most efficient method to reduce speckle, but also the most expensive).

Images 13, 14, 15 and 16 show the effect of parameter μ on the restoration process. The larger μ is, the more v contains information, and therefore the

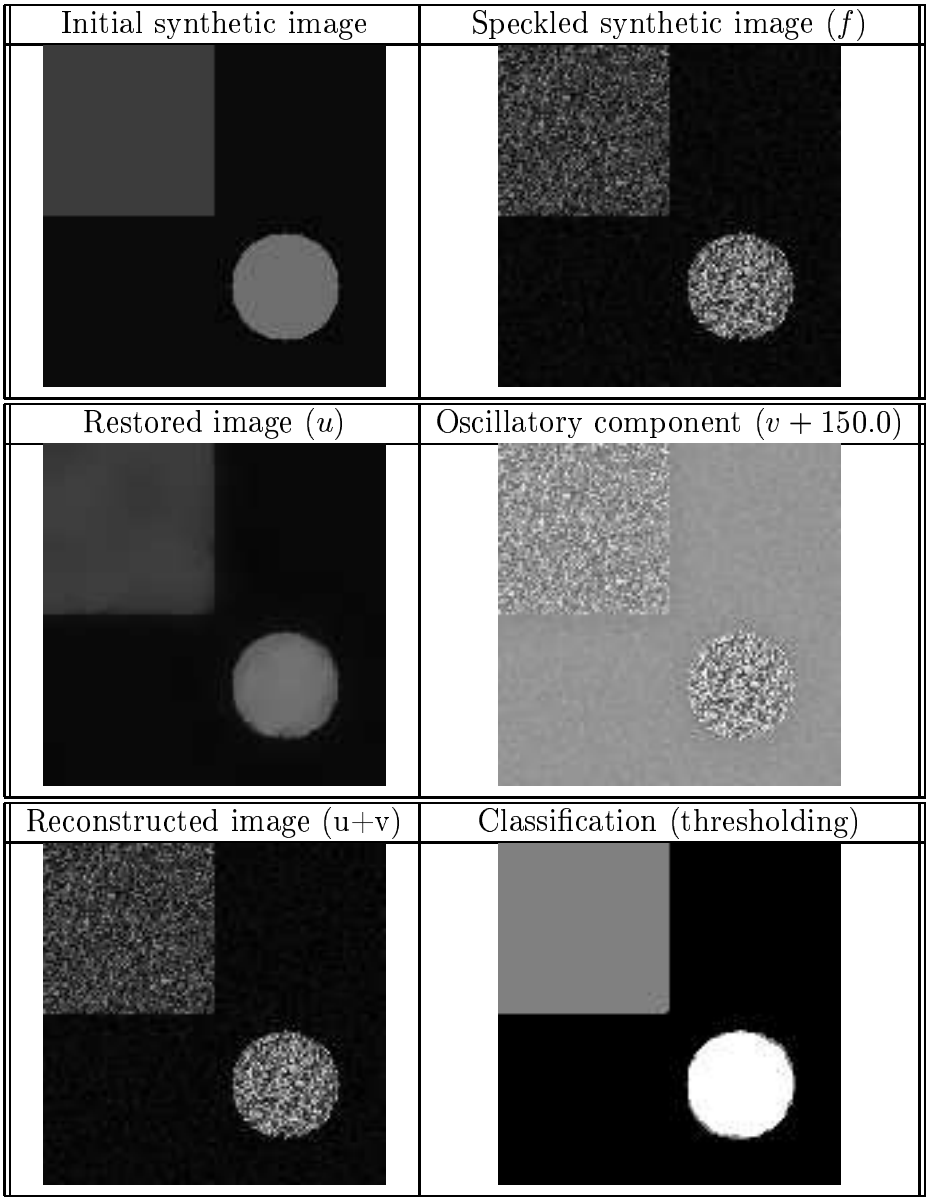

Figure 10: Simple synthetic image ($\lambda = 0.01$ and $\mu = 80$)

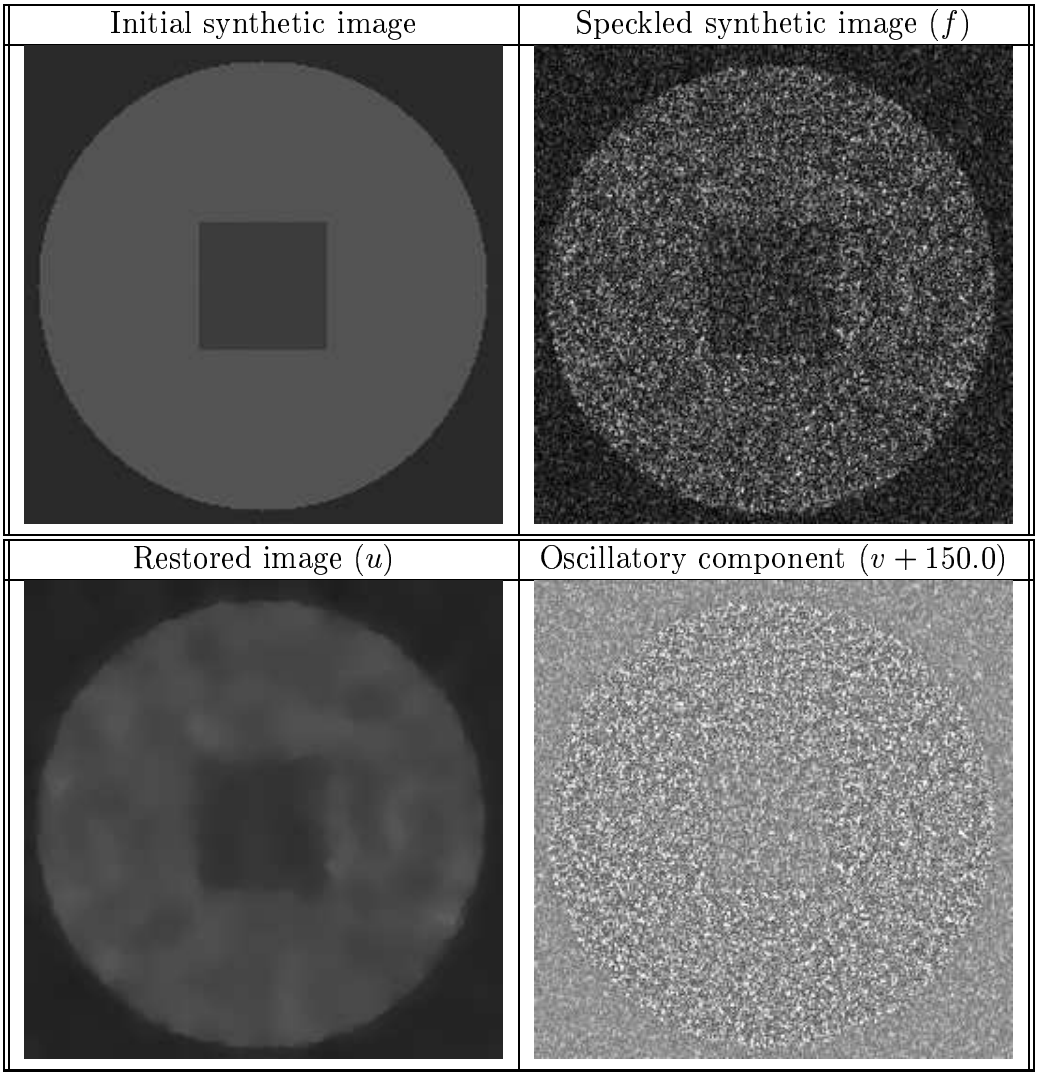

Figure 11: Complex synthetic image ($\lambda = 0.01$ and $\mu = 80$)

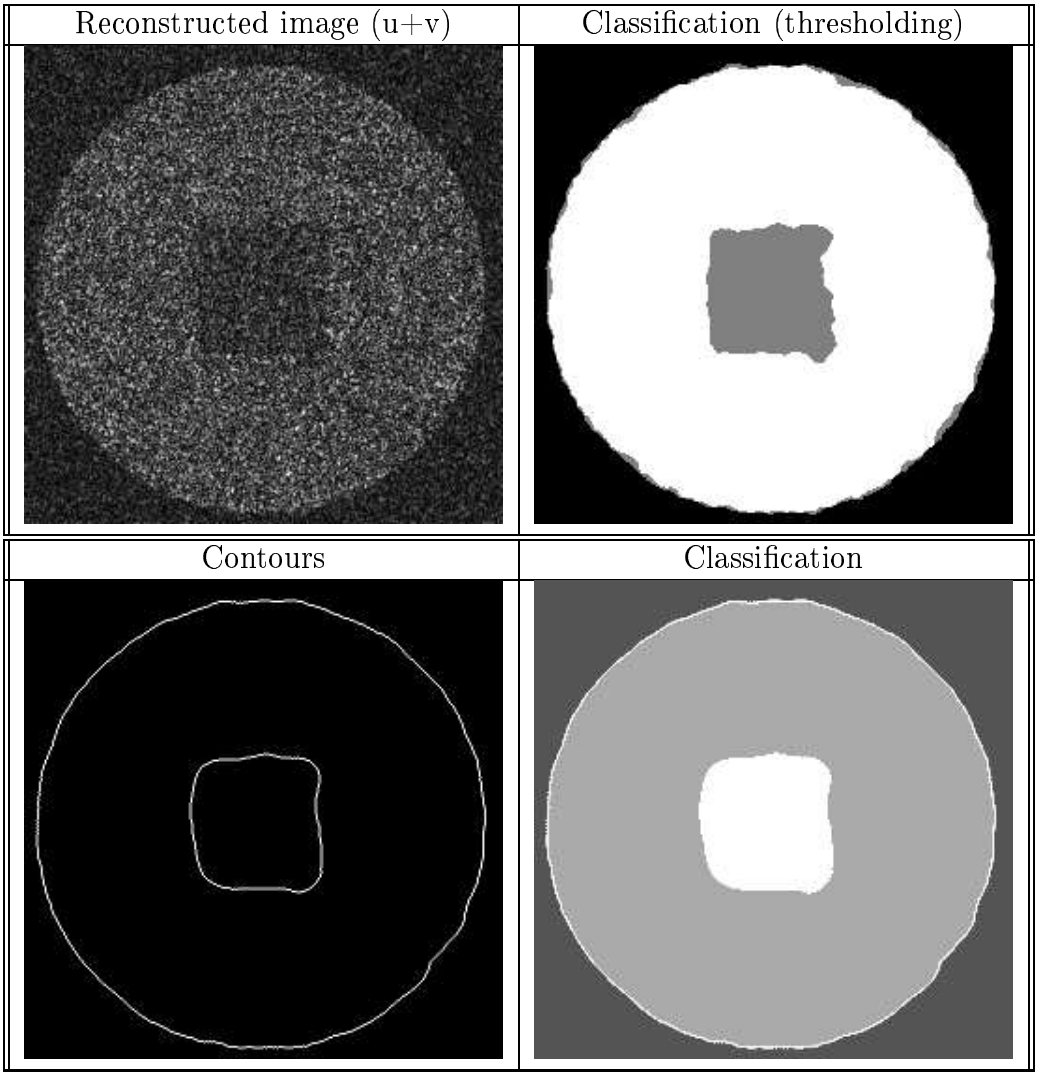

Figure 12: Complex synthetic image ($\lambda = 0.01$ and $\mu = 80$): classification

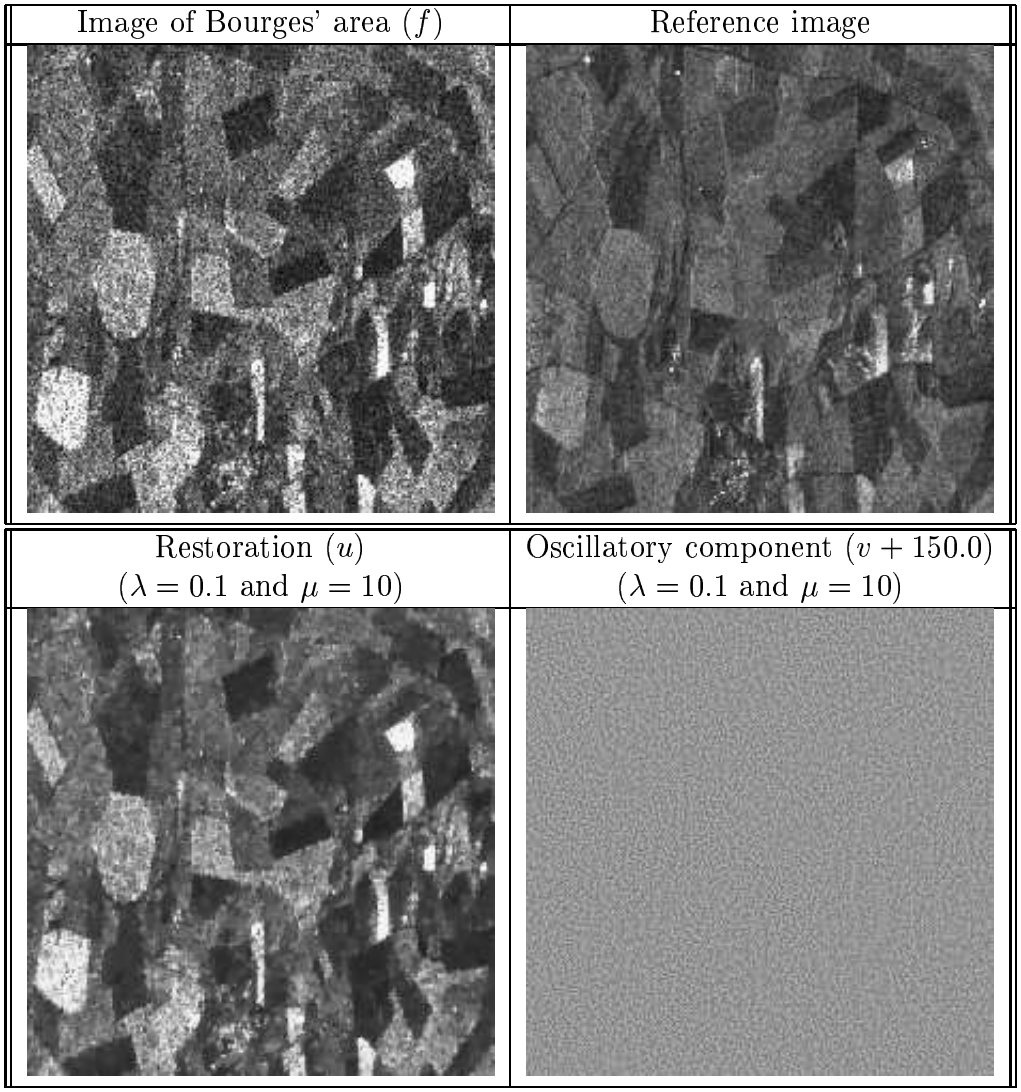

Figure 13: Image of Bourges' area 1

more u is averaged. According to the value of μ, we can thus get a more or less restored image, and also more or less smooth.

Here, the classification images are get through thesholding.

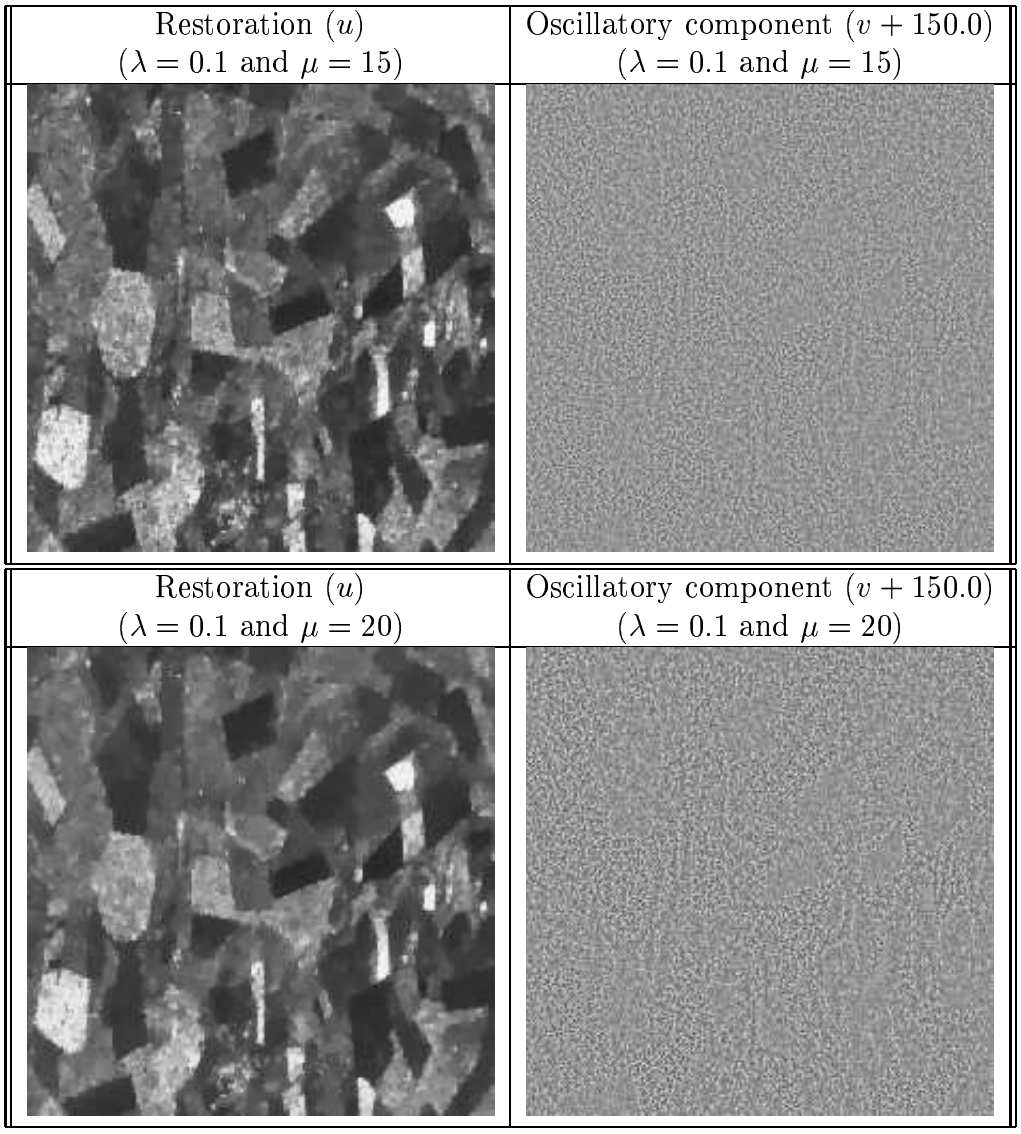

Figure 14: Image of Bourges' area 2

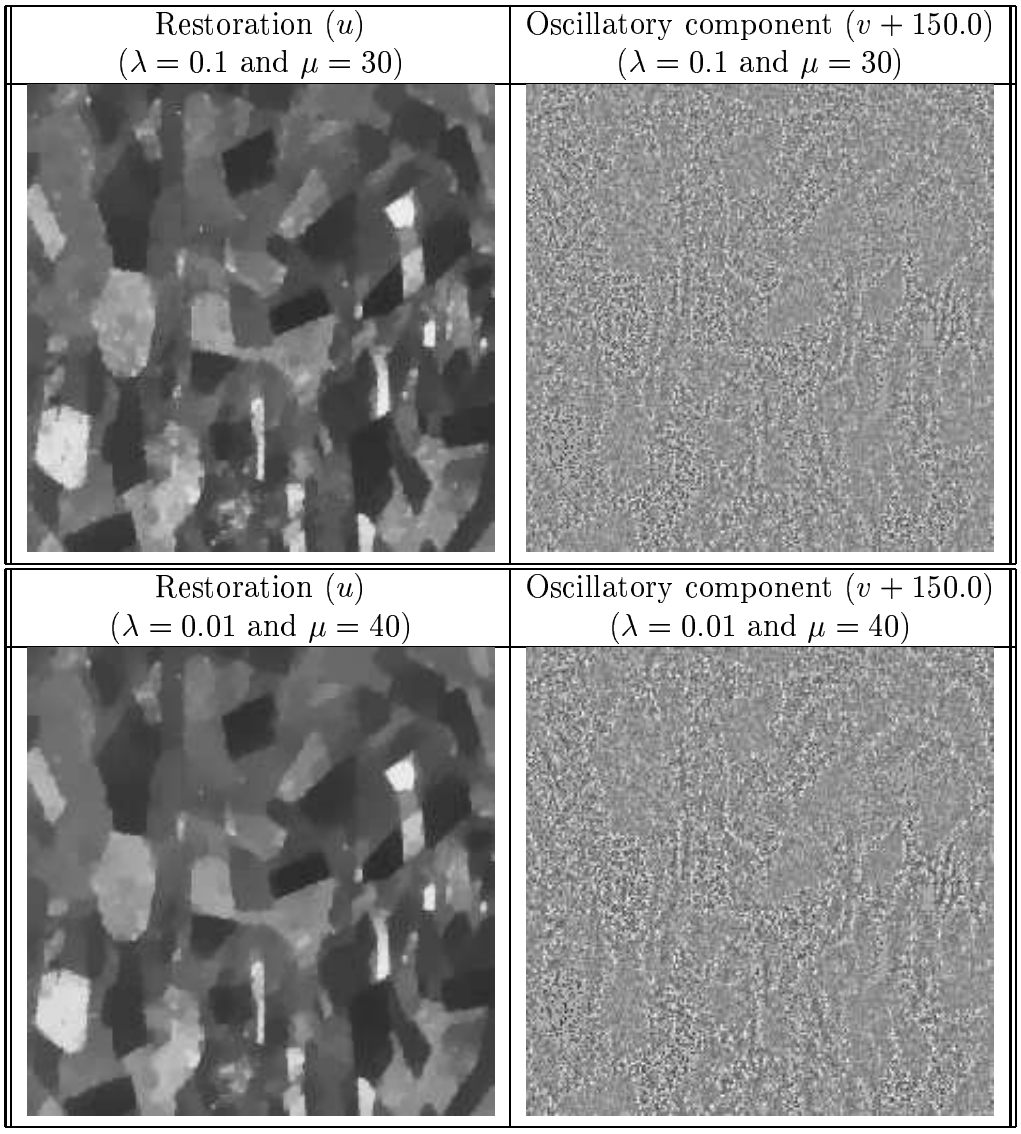

Figure 15: Image of Bourges' area 3

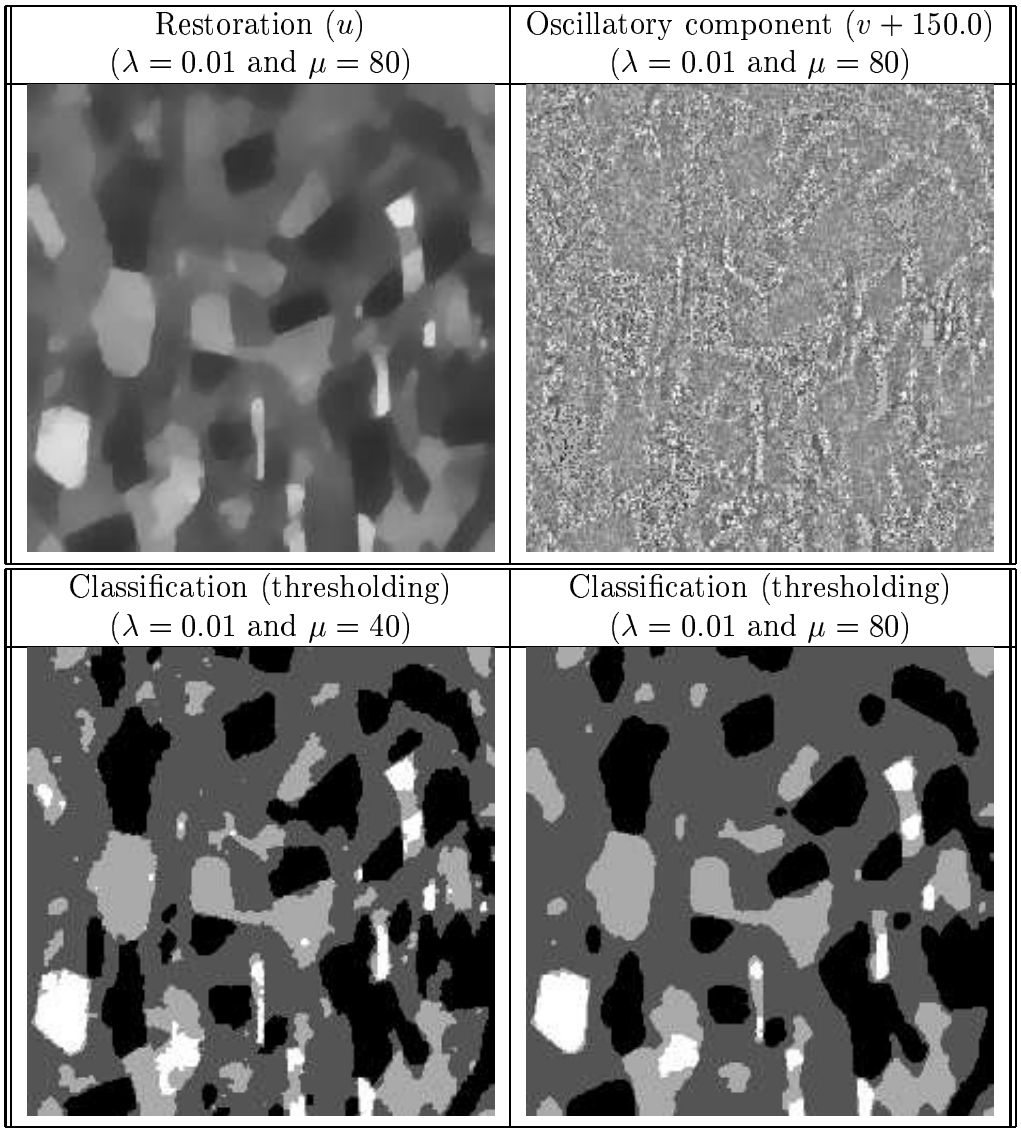

Figure 16: Image of Bourges' area 4

7. Conclusion

In this report, we present a new algorithm to decompose a given image f into a component u belonging to BV and a component v containing the noise and the textures of the initial image. Our algorithm performs Meyer's program [9]. We use the space G and its norm, and not an approximation as done in [17, 11]. Moreover, we carry out the mathematical study of our model. We show how the components u and v can be used respectively for textured images classification and for SAR images retoration. This last application appears to be very promising.

Acknowledgement: The authors would like to thank the French Space Agency CNES (Centre National d'Etudes Spatiales) and the French research center CESBIO (Centre d'Etudes Spatiales de la Biosphère) for providing real SAR data extracted from the CD-ROM *Filtrage d'images SAR* (1999). Part of this work has been funded by GdR-PrC ISIS through the young researcher program.

References

[1] L. Alvarez, Y. Gousseau, and J.M. Morel. Scales in natural images and a consequence on their bounded variation norm. In *Scale-Space '99*, volume 1682 of *Lecture Notes in Computer Science*, 1999.

[2] J.F. Aujol, G. Aubert, and L. Blanc-Féraud. Supervised classification for textured images, 2002. INRIA Research Report 4640.

[3] A. Chambolle. An algorithm for total variation minimization and applications, 2003. To appear in JMIV.

[4] A. Chambolle and P.L. Lions. Image recovery via total variation minimization and related problems. *Numerische Mathematik*, 76(3):167–188, 1997.

[5] I. Ekeland and R. Temam. *Analyse convexe et problèmes variationnels*, volume 224 of *Grundlehren der mathematischen Wissenschaften*. Dunod, second edition, 1983.

[6] J.B. Hiriart-Urruty and C. Lemarechal. *Convex Analysis ans Minimisation Algorithms I*, volume 305 of *Grundlehren der mathematischen Wissenschaften*. Springer-Verlag, 1993.

[7] D.C. Munson Jr and R.L. Visentin. A signal processing view of strip-mapping synthetic aperture radar. *IEEE Transactions on accoustics, speech, and signal processing*, 37(12):2131–2147, December 1989.

[8] Henderson Lewis. *Principle and applications of imaging radar*, volume 2 of *Manual of Remote Sensing*. J.Wiley and Sons, third edition, 1998.

[9] Yves Meyer. Oscillating patterns in image processing and in some nonlinear evolution equations, March 2001. The Fifteenth Dean Jacquelines B. Lewis Memorial Lectures.

[10] J.M. Nicolas, M. Sigelle, C. Thuillier, and F. Tupin. Images de radar à ouverture synthétique: transformée de Mellin et multirésolution. In *Seizième colloque GRETSI*, pages 797–800, September 1997.

[11] S.J. Osher, A. Sole, and L.A. Vese. Image decomposition and restoration using total variation minimization and the H^{-1} norm, October 2002. UCLA C.A.M. Report 02-57.

[12] T. Rockafellar. *Convex Analysis*. Etudes Mathématiques. Princeton University Press, 1974.

[13] L. Rudin, S. Osher, and E. Fatemi. Nonlinear total variation based noise removal algorithms. *Physica D*, 60:259–268, 1992.

[14] C. Samson, L. Blanc-Feraud, G. Aubert, and J. Zerubia. A level set method for image classification. *IJCV*, 40(3):187–197, 2000.

[15] F. Tupin. *Reconnaissance de formes et analyse de scènes en imagerie radar à ouverture synthétique*. PhD thesis, Ecole Nationale Supérieure des Télécommunications, Septembre 1997.

[16] M. Tur, C. Chin, and J.W. Goodman. When is speckle noise multiplicative? *Applied Optics*, 21(7):1157–1159, April 1982.

[17] Luminita A. Vese and Stanley J. Osher. Modeling textures with total variation minimization and oscillating patterns in image processing, May 2002. UCLA C.A.M. Report 02-19.

Unité de recherche INRIA Sophia Antipolis
2004, route des Lucioles - BP 93 - 06902 Sophia Antipolis Cedex (France)

Unité de recherche INRIA Lorraine : LORIA, Technopôle de Nancy-Brabois - Campus scientifique
615, rue du Jardin Botanique - BP 101 - 54602 Villers-lès-Nancy Cedex (France)
Unité de recherche INRIA Rennes : IRISA, Campus universitaire de Beaulieu - 35042 Rennes Cedex (France)
Unité de recherche INRIA Rhône-Alpes : 655, avenue de l'Europe - 38330 Montbonnot-St-Martin (France)
Unité de recherche INRIA Rocquencourt : Domaine de Voluceau - Rocquencourt - BP 105 - 78153 Le Chesnay Cedex (France)

Éditeur
INRIA - Domaine de Voluceau - Rocquencourt, BP 105 - 78153 Le Chesnay Cedex (France)
http://www.inria.fr
ISSN 0249-6399